Title
THERMODYNAMIC AND TRANSPORT PROPERTIES OF CeCu6

Author
Amato, A.

Publication Date
1987-02-01

LBL-22942
Preprint

Lawrence Berkeley Laboratory
UNIVERSITY OF CALIFORNIA

Materials & Molecular Research Division

Submitted to Journal of Low Temperature Physics

THERMODYNAMIC AND TRANSPORT PROPERTIES OF $CeCu_6$

A. Amato, D. Jaccard, J. Flouquet, F. Lapierre, J.L. Tholence, R.A. Fisher, S.E. Lacy, J.A. Olsen, and N.E. Phillips

February 1987

Prepared for the U.S. Department of Energy under Contract DE-AC03-76SF00098

DISCLAIMER

THERMODYNAMIC AND TRANSPORT PROPERTIES OF $CeCu_6$

A. AMATO and D. JACCARD

Département de Physique de la Matière Condensée, Université de Genève, 24 Quai Ansermet, 1211 Genève, Switzerland

J. FLOUQUET, F. LAPIERRE and J. L. THOLENCE

CRTBT-CNRS, BP 166 X, 38042 Grenoble-Cédex, France

R. A. FISHER, S. E. LACY, J. A. OLSEN and N. E. PHILLIPS

Materials and Molecular Research Division, Lawrence Berkeley Laboratory and Department of Chemistry, University of California, Berkeley CA 94720 USA

ABSTRACT

Measurements of the specific heat, magnetization and transport properties (resistivity, thermoelectric power and thermal conductivity) of single crystal $CeCu_6$ are reported with special emphasis on the effect of magnetic field. The relative field variations of the differential susceptibility, the coefficients of the linear temperature term of the specific heat and the T^2 resistivity term are presented. They are directly related to the field curvature of the magnetization, indicating the itinerant nature of the f-electrons. The Wilson ratio reaches a maximum at $H = H^*$, which may correspond to a crossover from a low field phase in which antiferromagnetic correlations dominate, to a highly polarized phase in which they are suppressed. Intersite coupling seems to play an important role in heavy-fermion compounds. Another interesting result is the occurrence of residual positive magnetoresistivity which also appears to be a general feature of heavy-fermion compounds. The properties of $CeCu_6$ are compared to those of other f-instability compounds and to present theories.

1. INTRODUCTION

The study of the normal phase of heavy-fermion compounds (HFC) may lead to a better understanding of the problem of interacting particles.[1] Because of the low symmetry (less than cubic) of the majority of HFC, it is important to perform experiments on single crystals. However, metallurgical difficulties have precluded such measurements on the two prototype Ce-based HFC, $CeAl_3$[2] and $CeCu_2Si_2$[3]. The virtual impossibility of growing a sufficiently large single crystal of $CeAl_3$ has restricted the analysis to crude theoretical models and has consequently limited the information obtained on magnetic correlations. The interest in $CeCu_6$ as a HFC was generated by the determination of a large value (1.6 $Jmole^{-1}K^{-2}$) of the coefficient of the linear temperature term (γ) of the specific heat.[4,5] The possibility of growing large single crystals allows more complete and systematic measurements and the correlation of macroscopic and microscopic properties.[6] We will describe transport, magnetization (M) and specific heat measurements (C) on several pieces of the same large single crystal. Special attention was given to the study of the action of an applied magnetic field (H) since it was thought that a high degree of magnetic polarization would lead to a state in which the interactions between particles was dominated by the interaction with H.

2. EXPERIMENTAL MEASUREMENTS

2.1. Sample Characterization

A single crystal of $CeCu_6$ was grown by the Czochralski method using a tungsten crucible under a high purity argon atmosphere. Its quality was checked by X-ray and neutron diffraction experiments. The residual resistivities [$\rho(0)$] are far lower than the resistivity maximum (ρ_{max}) reached for T ~ 9K; for example, along the $\underline{a}$ axis, $\rho_a(0) \sim 15$ $\mu\Omega$cm, $\rho_{max} \sim 82$ $\mu\Omega$cm; while along the $\underline{c}$ axis, $\rho_c(0) \sim 8$ $\mu\Omega$cm.[7] These results contrast with those for another single crystal of $CeCu_6$, also grown from a tungsten crucible,

for which ρ_0 reached a value[6] of 100 μΩcm. It has been suggested that better quality samples can be obtained from a boron nitride crucible[8], but it is shown here (as well as for samples recently prepared for magnetoresistivity and de Haas-van Alphen experiments for which $\rho_0 \sim 1$ μΩcm along the c axis[9]) that the nature of the crucible is not responsible for the lower resistivity ratio found in Ref. 8. ($CeCu_6$ has an orthorhombic structure at room temperature but exhibits a phase transition[10] near 200K to a monoclinic structure with a small distortion of about 1.5°. Here, the orthorhombic notation is retained.)

Resistivity (ρ) and thermoelectric power (Q) measurements have previously been reported for electric current (I) and temperature gradient (ΔT) applied along the three principal axes.[7] In this work, the magnetic field dependences of ρ, Q and K were measured with I and ΔT applied only along the a axis.[11] Q measurements were restricted to H ∥ a, while magnetoresistivity data were measured with the field oriented along the a, b and c axes. The thermal conductivity (K) was measured simultaneously with Q over a temperature range 40mK - 4K, and to 60 kOe. Specific heat and susceptibility (χ) measurements were made on the same single crystal sample of approximately cubic shape (3x3x3 mm^3). The cube and crystal axes coincided to better than 1°. At H=0, C was measured down to 50mK, but only down to 350mK in fields to 75 kOe. Magnetization measurements were performed in low fields (H < 2 kOe) from 40mK to 4.2K, and extended to 300K in fields to 50 kOe using a SHE SQUID magnetometer. High field measurements were made to 180 kOe between 1.6 and 4K at the "Service National des Champs Intenses".

2.2. Magnetization

Below 5K, remanent components (~0.8 emu/mole) were found in zero field after cycling to 50 kOe. The detection of a weak remanence is

common in HFC.[12] It does not seem to be correlated with long range ordering. Its occurrence may be due to a low content of parasitic magnetic phases or to the formation of magnetic clusters associated with lattice imperfections. For $CeAl_3$, it was clearly shown that the main origin of the remanence was the low content of the parasitic phases $CeAl_2$ and Ce_3Al_{11}, which order magnetically at 3.8K for $CeAl_2$ and at 6 and 3.2K for Ce_3Al_{11}.[2] For $CeCu_6$, the adjacent phase ($CeCu_5$) becomes antiferromagnetically ordered below[13] $T_N \sim 3.9K$; thus, the detection of a very weak remanence below this temperature might be due to lattice defects. χ was calculated from differences between zero (remanent) and finite field signals.

Figure 1 shows χ^{-1} vs T from 2 to 300K for the three principal axes. Similar curves were obtained for the samples used in transport measurements. The crossing of χ_a and χ_b occurs at 50K. The minimum of χ_b and the deviation of χ_a from its high temperature Curie-Weiss law, $\chi = \mu^2_{eff}/3k_B[T+\theta]$, occur at 10K. Below 50K, χ disagrees with the data of Ref. 14 but is in good agreement with that of Ref. 15. Fits by the Curie-Weiss law at high temperature (60-300K) lead to effective moments equal to 2.53, 2.62 and 2.44 μ_B and θ equal to 66, 70 and 9K along the a, b and c axes, respectively. The remarkable feature is that, along the easy magnetization axis, c, χ follows a Curie-Weiss law from room temperature to 80mK, the lowest experimental temperature. It should be noted that $T \sim 9K$ is the temperature at which χ_a and χ_b exhibit a change in their temperature dependences. χ^{-1} vs T below 5K is shown in Fig. 2. Extrapolated zero temperature susceptibilities are: $\chi_a(0) = 0.014$, $\chi_b(0) = 0.0096$ and $\chi_c(0) = 0.077$ emu mole^{-1}. By using the Maxwell relation

$$[\partial(C/T)/\partial H]_T = [\partial^2 M/\partial T^2]_H \qquad (1)$$

and the field dependence of C, the temperature dependence of M can be derived after integration. The dashed line in the lower part of Fig. 2 shows the temperature dependence of χ deduced from C(H). Excellent agreement is found with the susceptibility measurements. The low field dependence of M at low temperature is shown in Fig. 3. The linearity of M with H along the c axis contrasts with the behavior for H along the b axis. Low values of M in this direction increase the sensitivity of χ^{-1} to parasitic paramagnetic impurities as shown in the upper part of Fig. 2. High field measurements at 1.6K are plotted in Fig. 4. In contrast to HFC like UPt_3, $CeAl_3$ and $CeRu_2Si_2$,[16] which have positive curvature of M vs H, a negative curvature is observed along the c axis, while M is linear with H along the a and b axes. Taking into account the rather weak temperature dependence of M, we can assume that the zero temperature magnetization curve can be approximated by M(1.6K). The differential susceptibility,

$$\chi_H \equiv (\partial M/\partial H)_T, \tag{2}$$

is of interest since its field dependence can be compared to that of γ.

2.3. Specific Heat

At H=0 the temperature variation of C/T for 50mK < T < 20K shows three main regimes (see Fig. 5 and also Ref. 17): i) Above 10K, one observes the usual decrease with decreasing T. ii) There is a temperature interval (10 - 5K) of weak temperature dependence. iii) Below 4K there is an enormous increase of C/T with decreasing T. Experiments performed on sample G2 annealed 10 days at 680°C with a ρ_0 one half that of sample G1, led to similar results (insert of Fig. 5). In the very low temperature regime (T < 700mK) C/T can be fitted by the linear relation

$$C/T = 1.67 - 0.67T \text{ Jmole}^{-1}\text{K}^{-2}. \tag{3}$$

The absence of a maximum in C/T agrees with the results of Refs. 18 and 19 but not with those of Ref. 5. Such a discrepancy could originate in

the quality of the sample. Unfortunately, there is no indication in Ref. 5 of other measurements to check the sample quality. The weak temperature variation of C/T between 5 and 10K can be regarded as characteristic of an intermediate regime where the occurrence of the f-electrons in a renormalized band must be considered (in agreement with the observation of the resistivity maximum at 9K), but the large entropy, which is still present, leads to a strong decoupling of the electrons involved in the interactions. The mean value of C/T in this region, which we represent by γ_B, is 350 mJmole^{-1}K^{-2}, and is used as the normalizing factor when the field and temperature variation of C/T as T → 0 K are evaluated.

The temperature variation of C/χT normalized by the free electron ratio, $\pi^2 k_B^2/3\mu_B^2$, where χ is the average susceptibility, $\chi = (\chi_a + \chi_b + \chi_c)/3$, is shown in Fig. 6. At T=0, C/χT extrapolates to 0.68, i.e., between the free electron value 1 and the Wilson number 0.5. In Fig. 7, field dependences of C/T are plotted for H applied along the a, b and c axes. As mentioned in Ref. 5, large field-induced decreases of C/T are observed for H ∥ c. At H = 75 kOe, $\gamma = (C/T)_{T=0} \sim 500$ mJmole^{-1}K^{-2} and approaches γ_B. The occurrence of a maximum in C/T in high fields (H > 50 kOe) can be explained by the effect of the strong polarization of a narrow band with Zeeman decoupling between spin-up and spin-down bands at large H. This mechanism dominates the interaction between particles which, however, may decrease in high fields. The insert in Fig. 7 shows that, at 0.4 and 1K, C/T has an initial quadratic dependence on H even for large changes of C/T relative to $(C/T)_{H=0}$. For example, at 0.4K, the linearity in H is observed to 45 kOe where $(C/T)_H/(C/T)_{H=0} = 0.60$. The coefficients, α, of the H^2 law,

$$(C/T)_H = (C/T)_{H=0} - \alpha H^2, \qquad (4)$$

are 0.028 and 0.0107 JK^{-2}mole^{-1}T^{-2} for T = 0.4 and 1K, respectively. In the insert of Fig. 7 the similarity between the field dependence of C/T at 0.4 and 1K above H ~ 45 kOe should be noted.

Qualitatively, the anisotropy in C/T reflects that in the susceptibilities χ_a, χ_b and χ_c. We will discuss this point in more detail below.

2.4. Magnetoresistivity

Zero field resistivity data along the three principal axes have been reported previously.[4,7] Large anisotropies are found in the AT^2 and BT terms of ρ as well as in ρ_0.[7] A maximum in the scattering does not occur when current is applied along the c axis, but does occur when it is applied along a: $A_a \sim 122\mu\Omega cmK^{-2}$, $B_a = 37\mu\Omega cmK^{-1}$. Figures 8, 9 and 10 show, at different temperatures, the magnetoresistivity curve for H ∥ a, b and c axes, respectively. The a axis was therefore chosen for the current flow. At very low temperatures, an initial positive magnetoresistivity is observed for the three axes, whereas on warming, the usual negative magnetoresistivity, characteristic of local magnetic moments, is slowly recovered. Note that: i) At very low temperatures positive magnetoresistivity persists for H ∥ a and b to the highest field, 60 kOe, while for H ∥ c, a maximum in $\rho(H)$ appears at 15 kOe. ii) Negative magnetoresistivity is recovered in high fields for each axis, but more rapidly for H ∥ c.

For H ∥ c, we analyze the low temperature dependence of ρ for 0, 15 and 46 kOe. As shown in Fig. 11, for these field values, $\rho(H)$ can be fitted by the sum of a residual resistivity $\rho_0(H)$ plus a T^2 term

$$\rho(H) = \rho_0(H) + A(H)T^2. \qquad (5)$$

While $\rho_0(H)$ increases initially with H, A(H) decreases continuously in agreement with the reported decrease of $\gamma(H)$. Furthermore, the temperature range of the validity of the T^2 law ($T < T^*$) increases as A(H) decreases. The large anisotropy of ρ_0 and its field dependence suggest a contribution governed by f-electrons. It is noteworthy that the field variation of $\rho_0(H)$ up to its maximum is of the order of $A(H)T^{*2}$ (1-2μΩcm). The decomposition

of $\rho(H)$ into two terms implies a model where one type of carrier is scattered by two independent mechanisms. In the two-band picture[20,21] the itinerant electrons are strongly scattered by heavy particles through a Baber mechanism and by defects, which leads to a positive magnetoresistivity due to the deflection of the itinerant electrons by the applied field. In the first process, the resistivity is related to the square of the density of states of the heavy particles,

$$\rho_{ee} \sim N^2(\varepsilon_F)(k_B T)^2, \qquad (6)$$

i.e., in this crude model to γ^2. This leads to a proportionality between $A(H)$ and γ^2. In reality, the 4f-electrons and itinerant electrons (for example 5d) are hybridized leading to Bloch wave functions with mainly f and d character. On cooling, the transfer of heavy electrons to the light band becomes less and less probable, while the light electrons are strongly scattered.[22] The quasi-proportionality between $A(H)$ and γ^2 or $B(H)$ and γ have been determined experimentally.[23,24]

2.5. Thermal Conductivity

The thermal conductivity and the resistivity, measured with I and ΔT applied along a, are plotted in Fig. 12. A maximum in K appears centered around 300mK. The insert gives the L/L_0 ratio where L is defined by $L = K\rho/T$ and $L_0 = (\pi^2/3)(k_B/e)^2$ is the free electron value, 2.45×10^{-8} $W\Omega K^{-2}$.

At very low temperatures, $L = L_0$ indicating a negligible phonon contribution, i.e., K is dominated by the electronic contribution (K_e). Assuming a relation between ρ and K_e given by a Wiedemann-Franz like law, $K\rho/T \sim L$. When ρ has a dominant quadratic temperature dependence, a $K_e \sim 1/T$ law is expected.[25,26] However, below 100mK, the residual reistivity is large and K_e has the usual T variation ($K \sim L_0 T/\rho_0$) observed for electronic transport limited by impurities ($\rho_0 \gg AT^2$). The electronic contribution, assuming $L = L_0$, is shown as a dashed line in Fig. 12.

Above 0.2K (where ρ deviates from a T^2 dependence) $L > L_0$. This reflects the appearance of a supplementary contribution to K. Above 1K the thermal conductivity is linear in T, as observed in $CeAl_3$[25], in $CeCu_2Si_2$[27] and in polycrystalline $CeCu_6$[28]. A field sweep of K at 287mK shows a continuous and weak increase of K with increasing H (see Fig. 13) in qualitative agreement with the small negative magnetoresistivity shown in Fig. 8.

Thermal conductivity measurements have been reported previously[28] for a polycrystalline sample which had a rather large $\rho_0 \sim 32\mu\Omega cm$. A value of L/L_0 of 2.2 at very low temperature led to the conclusion that even as $T \to 0$ K, a phonon contribution (K_{ph}) comparable to the electronic one was present. In alloys, where the electronic mean free path becomes smaller than the predominant phonon wavelength, a large phonon contribution proportional to ρ_0 and T has been predicted and observed.[29] Here the striking point is the excellent agreement between our K values and the previous measurements.[28] K is weakly dependent on ρ_0, and the difference in L/L_0 as $T \to 0$ K seems to reproduce the difference in ρ_0. It is thus not obvious in our experiments that the increase of L/L_0 from 1, observed above 200mK, characterizes the phonon contribution. With increasing T, the increase of the entropy of the f-electrons may lead to a slow decoupling between their translational and magnetic degrees of freedom. This can produce a new mechanism for heat transfer.[30]

2.6. Thermoelectric Power

The thermoelectric power (Q_a) is always positive (see Fig. 14). If $CeCu_6$ is classified as a quasi-integral valent cerium compound like $CeCu_2Si_2$, $CeAl_3$, $CeAl_2$, etc., it does not obey the empirical rule that, at low temperature, Q is positive for non-integral valent cerium compounds (e.g., $CeSn_3$, $CePd_3$) and negative on approaching the trivalent

configuration.[31,32] To date the very low temperature regime ($T < T^*$) characteristic of the coherent state has not been achieved. Just as a strong magnetic polarization of trivalent HFC induces a positive contribution in the thermoelectric power,[32] here the persistence of the positive sign may be connected with the microscopic nature of the magnetic correlations. Another possibility is that $CeCu_6$ is close to the situation in $CeSn_3$ and $CePd_3$, i.e., very near the entrance to the intermediate valence (IV) regime.

The temperature variation of Q defines a low temperature regime ($T <$ 250mK) with a very large linear slope ($\partial Q/\partial T \sim 50\mu V/K^2$) followed by a weaker linear regime at higher temperatures ($T <$ 800mK, $\partial Q/\partial T \sim 4\mu V/K^2$). A sweep of H applied along a at 287mK shows a strong decrease of Q above ~15 kOe (see Fig. 15). This large variation contrasts with the weak dependence of C/T observed for H ∥ a.

3. DISCUSSION

3.1. Zero-Field Properties

As already reported[30,33] for $CeAl_3$, measurements of transport and thermodynamic properties of $CeCu_6$ show a very low temperature regime ($T < T^*$) above which thermal excitations between the different bands lead to a recovery of the properties of individual f-centers (Kondo effect). In $CeCu_6$, depending on the measurements chosen to define T^*, different values can be found. In thermoelectric power and Hall effect measurements,[17,34,35] a change of regime is observed near 300mK; in specific heat experiments a linear dependence of C/T on T is observed below 700mK; in dynamic measurements, like NMR[36] or inelastic neutron spectroscopy,[36] a simple behavior seems to occur, respectively, near 200mK and well below 700mK. If the temperature limit of the validity of the T^2 resistivity law is used, $T^* \sim 120$mK is found.[7] Whatever criterion is used to determine T^*, the values are lower than the estimates of the Kondo temperature

($T_K \sim 3.9K$) made by attempts to fit the specific heat data[5], or the resistivity behavior by comparison[38,39] with dilute $(Ce,La)Cu_6$ alloys. The occurrence of two characteristic temperatures has been determined experimentally.[31,33,36] It might be argued that T* is a redundant parameter as it is well known that a simple regime is achieved for a Fermi-liquid, of Fermi-temperature T_F, only below $T_F/10$. However, the low temperature regime cannot be extrapolated from the behavior observed near T_K. It has been observed recently in neutron experiments[37] that paramagnetic scattering is strongly modified below 0.7K. The recorded spectra show a broadening of the quasi-elastic peak a 0.7 and 7K, well explained by a Lorentzian shape with a linewidth characteristic of some Kondo temperature. However, at 0.1K, the spectra are clearly inelastic.[37] To reconcile the NMR data with the observation of a Korringa law[36] (typical of a Fermi-liquid excitation) a narrow quasi-elastic line must persist at T = 0. These microscopic probes demonstrate the occurrence of two different regimes.

In $CeAl_3$, much attention has been given to the maximum in C/T at a temperature $T^* \sim 350mK$ since it corresponds to anomalies in thermal expansion[2], thermoelectric power and resistivity[30]. This has led to a model with a minimum in the density of states at the Fermi-level.[40] Such a representation is purely phenomenological, and it does not give any microscopic information on the nature of the coupling. The absence of a maximum in C/T for $CeCu_6$ shows that such a feature is not common to HFC; its occurrence may depend on the interactions between particles and particularly on the dependence of the static susceptibility on the wavevector q. Neutron experiments[37,41] show that in $CeCu_6$ the coupling between two sublattices is antiferromagnetic within the crystallographic cell.

For the two prototype non-magnetic heavy-fermion compounds $CeAl_3$ and

$CeCu_6$, a linear dependence of C/T on T, $C/T = \gamma + \beta T$, has been found with positive β for $CeAl_3$ ($C/T = 1.20 + 1.96T$ Jmole^{-1}K^{-2}) and negative β for $CeCu_6$ ($C/T = 1.67 - 0.67T$ Jmole^{-1}K^{-2}). (For non-HFC, it is interesting to note that a similar dependence of C/T on T has been observed[46] below the spin glass temperature of CuMn.) This linear T dependence of C/T is not predicted by theories as $T \to 0$ K.[42,45] It has been suggested[47] that such a dependence may indicate a crossover regime, and that very low temperatures must be achieved in order to observe theoretical predictions, i.e., $T^2 \ln T$ (characteristic for RPA-like bosons mediating the interactions[44]) or T^2 (Sommerfeld development) terms. This is supported by the rather low value of the characteristic temperatures, $T^* \sim 350$mK and 200mK for $CeAl_3$ and $CeCu_6$, respectively, and by the empirical rule that simple laws are generally found only below $T^*/10$, i.e., roughly below 30mK. It is, therefore, of interest to extend the specific heat experiments to lower temperatures.

As for nearly ferromagnetic systems or nearly antiferromagnetic systems[42,43], the βT term in C/T does not contribute to the electrical resistivity. The observation of a T^2 resistivity law and the observation of $A(H) \sim \gamma^2$, with $\gamma \sim T^{*-1}$ when $C \sim \gamma T$, leads to a proportionality between C and $T^*(\partial\rho/\partial T)$ as observed for an antiferromagnetic phase transition.[48] It would be worthwhile measuring the thermal conductivity on a sample of lower ρ_0 to establish the contributions of the AT^2 term of ρ and the $\gamma T + \beta T^2$ terms of C on the temperature dependence of the thermal conductivity. Recently, the thermal conductivity and the Lorentz number of heavy electrons in Ce compounds has been investigated with the use of the Anderson lattice model in the framework of the single site approximation.[49] These studies seem to reproduce rather well the situation for $CeAl_3$ (gap structure in C/T above the Fermi-level) but

do not describe as well the case for $CeCu_6$ (no observation of a gap structure in C/T). An interesting result is that Lorentz numbers greater than L_0 are obtained on the basis of a purely electronic origin.

3.2. Low-Field Properties

In agreement with the Maxwell relation Eq. (1), the weak negative curvature of χ corresponds to a decrease of γ with H. The finite value of $C/\chi T \sim 0.68$ at T = 0 K shows clearly that the compound is far from a ferromagnetic instability ($C/\chi T \to 0$) as observed for nearly-ferromagnetic systems.[42] For comparison, Table I lists the average susceptibility $\chi(0)$ (averaged over the different orientations), γ, the ratio $\gamma/\chi(0)$, and the Gruneisen parameter [$\Omega = -(\partial \ln T_0/\partial \ln V)$] for the characteristic temperature T_0 at zero pressure for non-magnetic HFC ($CeCu_6$, $CeCu_2Si_2$ and $CeRu_2Si_2$), for cubic long-range magnetically ordered heavy-fermion compounds ($CeAl_2$, $CeIn_3$ and $CePb_3$) and for intermediate valence compounds (IVC) ($CeBe_{13}$, $CeSn_3$ and $CePd_3$). (References can be found in Refs. 50, 51, 52, 53 and 54.) For non-magnetic HFC, T_0 is taken as T*, while for magnetically ordered HFC, T_0 is taken as T_N (the ordering temperature). Very large Gruneisen parameters indicate the proximity of electronic and magnetic instabilites. All non-magnetic HFC have very large Ω_{T*}; by contrast, IVC have a small positive Gruneisen parameter. Magnetically ordered Kondo lattices like $CeAl_2$ and $CeIn_3$ have, at P=0, a rather small Gruneisen parameter,[50] i.e., the appearance of the magnetic to non-magnetic transition is at much higher pressure (~30 kbar for $CeIn_3$[51]). $CePb_3$ seems closer to a magnetic instability than $CeAl_2$ and $CeIn_3$.[52]

Non-magnetic compounds (HFC or IVC) have rather similar values of $\gamma/\chi(0)$. However, there are difficulties in assigning a bare magnetic moment (m_0) to the particles (its magnitude may differ significantly from the 1 μ_B attributed to free electrons) and in taking into account the effects of the 2J+1 level degeneracy and of the anisotropy in the susceptibility, which preclude a detailed

discussion of $\gamma/\chi(0)$. In Ref. 2, an attempt was made to determine a Landau-like exchange parameter (F_0^a) through the relation

$$\gamma/\chi(0) = (\pi^2 k^2_B/m^2_0)[J/(J+1)]\ (1 + F_0^a). \qquad (7)$$

For $CeSn_3$ a prototype IVC, $F_0^a \sim -0.05$, while for $CeAl_3$ $F_0^a \sim -0.7$. This difference is in good agreement with a decrease of F_0^a with the increase of the degeneracy of the crystal field ground state.[1] However, the determination of F_0^a suffers from the uncertainties (anisotropy and evaluation of m_0) already mentioned.

Concerning the magnetic/non-magnetic duality in HFC, it is worth noting the case of $CeAl_2$ for which the ratio $\gamma/\chi(0)$ is far lower than the Wilson or free electron ratio, and that of $CePb_3$ for which $\chi(0)$, γ and $\gamma/\chi(0)$ have values typical of non-magnetic HFC. In $CeAl_2$, the main contribution to χ is from magnetically ordered 4f moments with a small contribution from itinerant 4f-electrons.[50] The localized character of the magnetism leads to a large decrease of χ below T_N as usually found for rare earth compounds. On the other hand, for $CePb_3$, the itinerant character of the f-electrons has drastically increased,[52] with χ showing only a small maximum at T_N. The similarity in the low temperature parameters of a magnetically ordered HFC like $CePb_3$ and non-magnetic HFC shows that, at low temperatures, there is no marked difference between non-magnetic and magnetic HFC. Similar remarks have been made concerning the values of the high temperature parameters for $CeAl_2$ and $CeAl_3$.[2,21] In both cases the RKKY interactions may compete equally with the Kondo coupling,[55] but the symmetry of the lattice seems to play a dominant role in preventing magnetic ordering.[2] The single site approximation, with vanishing coupling, seems appropriate only for IVC.[56,58]

3.3. High-Field Properties

In the field dependences of the transport and thermodynamic properties of $CeCu_6$, two characteristic regimes (below ~15 kOe and below ~45 kOe)

appear. For example, the magnetoresistivity at 40mK for H ∥ c (see Fig. 10) has a maximum at 15 kOe and a minimum at 40 kOe, and features appear in Hall effect measurements[35] at similar field values. A weak field dependence of Q occurs for H < 15 kOe along a. Specific heat measurements are linear in H^2 to 45 kOe for H ∥ c with no maximum in C/T. There is apparently no indication of changes in magnetic properties at these characteristic fields. However, for H = 45 kOe along c, a large magnetic polarization is achieved [M(45 kOe) ~ 0.5 μ_B].

Figure 15 shows the field dependence of $\gamma(H)$, $\chi(H)$ and $A(H)^{1/2}$ normalized to the zero field value $\gamma(0)$. Qualitatively $\gamma(H)$, $\chi(H)$ and $A(H)^{1/2}$ have similar field variations but quantitative differences appear which may reflect the nature of the interactions. It is well established for nearly ferromagnetic systems that the paramagnon contributins to χ, C and ρ depend differently on the Stoner factor.[42,43] Here, the difficulty is in taking into account the role of the strong anisotropy. However, another indication of a "magnetic crossover" from low field to high field phases is given by the occurrence of a minimum in the ratio of $\gamma(H)/\chi(H)$ ~ 0.48 for H^* ~ 45 kOe. This characteristic field coincides with a change in the temperature dependence of C/T: the absence of a maximum below 45 kOe and the existence of a maximum above 45 kOe, which moves to higher temperatures as the field is increased. In agreement with the presence of these two domains, $\gamma(H)$ cannot be described by a unique formula. The dependence is less than that predicted by a Lorentzian variation

$$\gamma_L(H) = \gamma(0)/[1+\eta\gamma(0)H^2], \qquad (8)$$

which may describe the field shift of a narrow band of Lorentzian density of states centered at the Fermi-level. However, it is larger than that proposed previously,[41]

$$\gamma(H) = \gamma(0)/[1+\eta'\gamma(0)^2H^2]^{1/2}, \qquad (9)$$

where no shift is assumed with respect to the Fermi-level, but only a continuous broadening.[5] Applying a magnetic field results in a cancellation of the antiferromagnetic interactions between two next-nearest-neighbor atoms. A crossover field will separate a low field regime where the heavy particles strongly interact from a high field regime where the particles may be heavy by renormalization effects but their mutual interactions have collapsed.

As previously mentioned, two temperature regimes may appear in zero field. The non-interacting one ($T > 5K$) corresponding to a narrow band of independent particles, and the interacting one corresponding to the large increase of γ from γ_B, where the significant enhancement is $\gamma/\gamma_B \sim 4$ not $\gamma/\gamma_F \sim 200$ (γ_F being the term associated with free electrons in a $CeCu_6$ lattice). In this picture, to emphasize that when $\gamma \to \gamma_B$ the interaction has decreased, the field variation of γ has been parametrized by an interaction term $E_{int}(H)/E_0$ through the relation

$$\gamma/\gamma_B = 1/[1-E_{int}(H)/E_0], \qquad (10)$$

where E_0 is a constant critical energy parameter.

Taking into account the crudeness of the analysis, the change in slope of $E_{int}(H)/E_0$ for $H \sim 50$ kOe (see Fig. 16) can be correlated with the minimum in $\gamma(H)/\chi(H)$ at $H \sim 45$ kOe (see Fig. 15). For $CeRu_2Si_2$[16] or UPt_3[59], which have metamagnetic-like transitions at H^* equal to 80 and 210 kOe, respectively, enormous decreases of $\gamma(H^*)/\chi(H^*)$ have been observed. These marked effects in comparison to the small variations in $CeCu_6$ may reflect the nature of the antiferromagnetic coupling. The polarized paramagnetic phase above H^* may be achieved through a metamagnetic-like transition (in $CeRu_2Si_2$ and UPt_3) or a spin-flop like tansition in $CeCu_6$. By analogy to the H-T phase diagram for antiferromagnetic transitions, H^* and T^* define the limits of low- and high-field phases. Such a hypothesis should be tested in the future by neutron experiments.

3.4. Anisotropy

Qualitatively, the anisotropy in $\gamma(H)$ reflects that of the susceptibilities χ_a, χ_b and χ_c. However, for a quantitative calculation it is not obvious how to evaluate the necessary parameters. For example, the Zeeman energy of the particles, which can be used in the Lorentzian, Eq. (2), can be evaluated if we assume that the difference between $(C/T)_a$, $(C/T)_b$ and $(C/T)_c$ at constant field are due to the anisotropy of the g-factors. If the different values of $\chi_a(0)$, $\chi_b(0)$ and $\chi_c(0)$ correspond to different values of g, the Zeeman energy would be proportional to $\chi(0)^{1/2}$. Using $\gamma_L(H)=\gamma$, H = 75 kOe along a would correspond to H = 31 kOe along c. The observed effect is far greater along c than along a using such a scaling formula. Another simple assumption is that the predominant variable is the magnetization of the lattice, i.e., $M = \chi(0)H$ at T=0. With this hypothesis, the axial correspondence is better than before, but the deviation between the experimental data and this scaling is reversed compared to that found previously. For example, for 0.35K with 75 kOe along a, the relative decrease of C/T is 7.2%, but only 3.9% for the same polarization along c at 15 kOe. The large anisotropy of the resistivity may indicate mainly single ion anisotropic scattering as suggested by theory.[60,61] If the crystal field ground state is one of the highly anisotropic doublets, $J_z = \pm 3/2$ or $\pm 5/2$, no resistivity will occur along the c axis for infinite crystal field splitting.

3.5. Residual Magnetoresistivity

We have emphasized that the field dependence of the A(H) term of the resistivity is connected to that of $\chi(H)$ and $\gamma(H)$. When M(H) has an initial positive curvature with H, as for $CeAl_3$[60], $CeRu_2Si_2$[16] and UPt_3[59] $\gamma(H)$ and A(H) increase initially with H and their maxima coincide with that of $\chi(H)$ at H*. When M(H) has a continuous negative curvature

with H as for $CeCu_6$, $\gamma(H)$ and $A(H)$ decrease continuously with H. The field dependence of $\rho_0(H)$ is less trivial. An initial positive $\rho_0(H)$ appears to be a common feature of HFC since it is observed in $CeAl_3$, $CeRu_2Si_2$, UPt_3 and $CeCu_6$ whatever the sign of the curvature of M(H). UBe_{13} is the only example where negative residual magnetoresistivity has been found.[63] However, the reported negative $\rho_0(H)$ may be illusory since the appearance of superconductivity at $T_c > T^*$ (before the Fermi-liquid region is reached) rules out the observation of its low field behaviour in the normal phase below T*. For $CeAl_3$[62], $CeRu_2Si_2$[16] and UPt_3[59], the field maximum of $\rho_0(H)$ coincides with that of $\chi(H)$. For $CeCu_6$ the maximum of $\rho_0(H)$, observed with I along a and H along c at 15 kOe, does not coincide with a corresponding maximum for $\chi(H)$. Published data on a single crystal of comparable ρ_0, with the same field direction, but a current flow along b, shows a similar $\rho_0(H)$ with a maximum at 20 kOe and a minimum at 50 kOe.[38,39] Furthermore, our results suggest that the temperature (T_x), where at constant H the transverse magnetoresistivity changes its sign, is almost field independent below 15 kOe. This phenomenon, first reported for $CeAl_3$[64], was studied recently[38,39] in $CeCu_6$.

3.6. Comparison with Theory

The occurrence of two temperature regimes (T_K,T*) in non-magnetic HFC have been emphasized theoretically.[65,66,68] A new study of the Anderson lattice, by making a loop correction due to spin-fluctuations to the f-electron self-energy, has found a sharp peak in the spectral density corresponding to heavy quasi-fermions, and a broad peak similar to the Kondo resonance in a Kondo impurity.[68] As the temperature increases, the quasi-fermion peak diminishes and changes into the resonance peak as found previously.[65,67] This scheme is qualitatively in good agreement with reported NMR and inelastic neutron experiments. No q-dependence of the static susceptibility is given.

A T^2 resistivity law in ordinary metals can be explained by different mechanisms,[69] which may also be used for HFC. We have previously referred to the two-band model[20,21] developed around 1936. In this picture, the hybridization between the two bands is neglected, and the Coulomb interaction between light and heavy particles leads to the T^2 variation of ρ via the Baber mechanism.[21] (However, it has been argued that a two-band model is an incorrect picture at very low temperatures.[70]) The first calculation for a Kondo lattice was made by assuming a wavevector dispersion for the f-electron band in order to avoid a gap opening. It was emphasized that $\rho \sim (T/T_K)^2$. However, the proportionality constant is not universal but depends on the band structure. This model was recently extended on the basis of the coherent potential approximation, and applied to heavy electrons in alloys.[72] Calculations for a Kondo lattice, assuming a linear T variation of the mean square of the fluctuating potential, have shown a linear T/T_K resistivity term with γ inversely proportional to the Kondo temperature.[73] Recently the fluctuation corrections to mean field theory applied to the $(T/T_K)^2$ resistivity law have been studied by 1/N expansion methods.[74,75,45,46] The proportionality of A and γ^2 has been strongly emphasized.[46] Fermi-liquid theory, on the basis of a periodic Anderson Hamiltonian, leads also to a linear T term for C and a T^2 term for ρ, with A proportional to γ^2 if the momentum conservation of the vertex part between antiparallel spins is ignored.[76] In agreement with electron-electron interactions for a spherical Fermi-surface, the coefficient A vanishes if there is no crystal lattice.

Calculations of the ratio γ/χ for a lattice have been given.[46,75,76,70] The theory based on a 1/N expansion[46,75] predicts that the Landau parameter $F_0^a \sim -1/N$ is identical to the one impurity Anderson model to leading order in 1/N. This result seems to be in good agreement with the

values of F_0^a calculated by Eq. (3), but it is not obvious that the theoretical expression[75] has the same prefactor for the derivation of F_0^a. The ratio γ/χ has been calculated recently[70] on the basis of a band model within the Korringa-Kohn-Rostoker scheme. Taking into account the fact that the magnetic moments of the heavy fermions are strongly reduced, since only one specific linear combination of the 2J+1 f-states can hybridize with a conduction band, it was predicted that the enhancement, $(1+F_0^a)^{-1}$, of the susceptibility over γ may always occur. This leads to the general idea that local spin-fluctuations are enhanced relative to the non-interacting Fermi-liquid. For $CeSn_3$, F_0^a will be equal to -0.5. This model corresponds to the fully degenerate J = 5/2 case, i.e., mostly to IVC. The absence of a theory taking into account crystal field splitting and band structure does not allow us to assign with confidence the variations in ferromagnetic or antiferromagnetic intersite couplings to the differences in the γ/χ values of Table I. However, it should be noted that $CeCu_6$ and $CeCu_2Si_2$ have a rather similar ratio. The relatively large γ/χ of $CeCu_2Si_2$ has been interpreted as indirect evidence of antiferromagnetic correlations.[19]

The quasi-proportionality of A and γ^2, and the weak deviation of γ/χ from free-electron or Wilson values, are characteristic of a smooth dependence of the static susceptibility [$\chi(q)$] and of the moment relaxation rate [$\Gamma(q)$] on the wavevector q.[42] The local character of the fluctuations is predominant. For nearly ferromagnetic systems, the different dependences of A, γ and χ on the Stoner factor are a consequence of the strong q dependence of χ and Γ. For example, $\Gamma(q) \sim q$ for nearly ferromagnetic systems,[42] while a weak dependence of $\Gamma(q)$ on q has been reported[41] for $CeCu_6$. Experimental data[23,24] show that the band structure and the crystal symmetry does not modify drastically the proportionality constant between A and γ^2.

Concerning the specific heat, few attempts have been made to obtain the supplementary βT^2 term, only the γT contribution, in the $T \to 0$ limit. An interpretation of the maximum in C/T observed in $CeAl_3$ has been given in terms of fluctuations of the spin density wave.[77] It has also been stressed that the $T^3 \ln T$ term of the specific heat must be observed as a general property[44,45] of HFC, not as evidence of a ferromagnetic instability.[45,46]

The action of a magnetic field on HFC has not been studied extensively. With the previously mentioned hypothesis of a gap structure of the Kondo resonance a little above the Fermi-level[78], positive magnetoresistivity has been calculated in the single site approximation. A similar result was derived in a molecular field treatment of the Kondo lattice.[73] The problem of residual resistivities has been ignored. It was pointed out recently[79] that in zero magnetic field only a small randomness exists in renormalized f-levels, even though a large randomness occurs in the hybridization between electrons near bare 4f-levels. The renormalized 4f-levels (host and impurities) are pinned at the chemical potential so long as the 4f occupancy numbers of spin-up and spin-down are equal to 1/2. The huge positive magnetoresistance is due to the strong increase of the randomness of the renormalized f-levels with H, which are no longer fixed at the Fermi-level. A magnetic field is a probe of the deviations of the Kondo temperature and local susceptibility apart from the lattice parameters. This origin of residual positive magnetoresistivity is quite different from that of usual metals, where it is due to the deflection of the itinerant electrons by a magnetic field. That leads to the Koehler rule, i.e., $\Delta\rho(H)/\rho_0 = f(H/\rho_0)$. Further experiments on different samples are needed to clarify in HFC the relation between $\Delta\rho(H)$ and ρ_0.

4. CONCLUSION

As observed for $CeAl_3$, very low temperatures must be achieved to observe the properties of the ground state of $CeCu_6$. Common features occur between normal phases of HFC but the occurrence of a maximum in the temperature variation of C/T or $\chi(T)$ may depend on the microscopic nature of the interactions between particles and particularly on their magnetic couplings. Similar remarks apply to the field dependence of γ or M. In $CeCu_6$, γ and χ seem to show a monotonous decrease with H, however, the ratio of γ/χ presents a well defined minimum for $H \sim H^* \sim 45$ kOe. It was emphasized that the low and high field phases may differ on both sides of H^*. These two regimes appear clearly in the temperature dependence of C/T. The similarity of HFC, whenever a long range magnetic order exists, as well as the role of the axial symmetry of the lattice in preventing magnetic ordering, were clearly demonstrated.

The strong scattering of the quasi-particles by impurities is clear in magnetoresistivity experiments. Residual positive magnetoresistivity seems a common feature in non-magnetic HFC. Further measurements on other examples with lower residual resistivity must be made in order to obtain the maximum amount of information available from experiments. This is particularly true for thermal conductivity experiments. Although, for example, there is no doubt that the change in the regime of the thermoelectric power is associated with the entrance to the low temperature heavy-fermion state, the determination of the intrinsic part is needed as well as the role of the impurities. The observation in non-magnetic HFC ($CeCu_6$, $CeAl_3$, $CeRu_2Si_2$ and UPt_3), that the field variation of γ and A is governed by the field curvature of M, demonstrates that the renormalized f-levels are at the Fermi-level.

ACKNOWLEDGEMENTS

We thank Prof. J. Sierro and E. Walker for stimulating discussions and also the growth of the single crystal (E.W.). One of us (J.F.) thanks the Japan Society for the promotion of Science for providing the opportunity to improve his understanding on HFC and particularly Prof. K. Asayama and Dr. Y. Kitaoka. The work at Berkeley was supported by the Director, Office of Energy Research, Office of Basic Energy Sciences, Materials Sciences Division of the U.S. Department of Energy under Contract DE-AC03-76SF00098.

REFERENCES

1. P.A. Lee, T.M. Rice, J.J. Sham and J.W. Wilkins, Comments Mat. Phys. 12, 99 (1986).

2. J. Flouquet, J.C. Lasjaunias, J. Peyrard and M. Ribault, J. Appl. Phys. 53, 2127 (1982). A. Benoit, A. Berton, J. Chaussy, J. Flouquet, J.C. Lasjaunias, J. Odin, J. Palleau and J. Peyrard, in "Valence Fluctuations in Solids", eds. L.M. Falicov, W. Hanke and M.B. Maple, North Holland, Amsterdam (1981).

3. See F. Steglich, "Theory of Heavy Fermions and Valences Fluctuations", eds. T. Kasuya and T. Saso (Springer-Verlag), (1985), p. 23.

4. G.R. Stewart, Z. Fisk and M.S. Wire, Phys. Rev. B30, 482 (1984).

5. T. Fujita, K. Satoh, Y. Onuki and T. Komatsubara, J. Magn. Magn. Mat. 47-48, 66 (1985). K. Satoh, F. Fujita, Y. Maeno, Y. Onuki, and T. Komatsubara, Solid State Commun. 56, 327 (1985).

6. Y. Onuki, Y. Shimizu and T. Komatsubara, J. Phys. Soc. (Japan) 53, 1210 (1984).

7. A. Amato, D. Jaccard, E. Walker and J. Flouquet, Solid State Commun. 55, 1131 (1985).

8. Y. Onuki, K. Shibutami, T. Hirai, T. Komatsubara, A. Sumiyama, Y. Oda, H. Nagano, H. Sato and K. Yonemitsu, J. Phys. Soc. (Japan) 54, 2804 (1985).

9. P.H.P. Reinders, M. Springford, P.T. Coleridge, R. Burlet and D. Ravot, "Proceedings of the International Conference on Anomalous Rare Earths and Actinides", Grenoble (1986), J. Magn. Magn. Mat., to be published. P.H.P. Reinders, M. Springford, P.T. Coleridge, R. Burlet and D. Ravot, in Phys. Rev. Lett. 57, 1631 (1986).

10. T. Suzuki, T. Goto, A. Tamaki, T. Fujimura, Y. Onuki and T. Komatsubara, J. Phys. Soc. (Japan) 54, 2367 (1985).

11. A. Amato, D. Jaccard, J. Sierro, E. Walker and J. Flouquet, "Proceedings of the International Conference on Anomalous Rare Earths and Actinides", Grenoble (1986), J. Magn. Magn. Mat., to be published.

12. J.L. Tholence, P. Haen, D. Jaccard, P. Lejay, J. Flouquet and H.F. Braun, J. Appl. Phys. 57, 3172 (1985).

13. E. Bauer, E. Gratz and C. Schnitzer, "Proceedings of the International Conference on Anomalous Rare Earths and Actinides", Grenoble (1986), J. Magn. Magn. Mat., to be published.

14. S. Zemirli and B. Barbara, Solid State Commun. 56, 385 (1985).

15. Y. Onuki, Y. Shimizu and T. Komatsubara, J. Phys. Soc. (Japan) 54, 304 (1985).

16. See P. Haen, J. Flouquet, F. Lapierre, P. Lejay and G. Remenyi, to be published in J. Low Temp. Phys.

17. T. Penney, J. Stankiewicz, S. Von Molnar, Z. Fisk, J.L. Smith and H.R. Ott, J. Magn. Magn. Mat. 54-57, 370 (1986).

18. H.R. Ott, H. Rudigier, Z. Fisk, J.O. Willis and G.R. Stewart, Solid State Commun. 53 235 (1985).

19. F. Steglich, U. Rauschwalbe, U. Gottwick, H.M. Mayer, G. Spain, N. Grewe, U. Poppe and J.J.M. Franse, J. Appl. Phys. 57, 3054 (1985).

20. N.F. Mott, Proc. Roy. Soc. (London) A 156, 368 (1936).

21. W.E. Baber, Proc. Roy. Soc. 258, 383 (1937).

22. L. Colquitt Jr., H.R. Frankhauser and F.J. Blatt, Phys. Rev. B4, 292 (1971).

23. B. Bellarbi, A. Benoit, D. Jaccard, J.M. Mignot and H.F. Braun, Phys. Rev. B30, 1132 (1984).

24. K. Kadowski and S.B. Woods, Solid State Commun. 58, 507 (1986).

25. H.R. Ott, O. Marti and F. Hulliger, Solid State Commun. 49, 1129 (1984).

REFERENCES (continued)

26. J. Flouquet, P. Haen, C. Marcenat, P. Lejay, A. Amato, D. Jaccard and E. Walker, J. Magn. Magn. Mat. 52, 85 (1985).

27. W. Franz, A. Griessel, F. Steglich and D. Wohlleben, Z. Phys. B31, 7 (1978).

28. Y. Peysson, B. Salce, C. Ayache and E. Bauer, J. Magn. Magn. Mat. 54-57, 423 (1986).

29. J.E. Zimmermann, J. Phys. Chem. Solids 11, 299 (1959).

30. D. Jaccard and J. Flouquet, J. Magn. Magn. Mat. 47-48, 45 (1985).

31. D. Jaccard and J. Sierro, "Valence Instabilities", eds. P. Watcher and H. Boppart, North Holland, Amsterdam (1982).

32. D. Jaccard, J. Sierro and J. Flouquet, J. Appl. Phys. 57, 3084 (1985).

33. J. Flouquet, Congres de la Societe Francaise de Physique 1983: "A Travers la Physique" (Les Editions de Physique) p. 293.

34. T. Penney, F.P. Milliken, S. Von Molnar, F. Holtzberg and Z. Fisk, to be published in Phys. Rev. B.

35. K. Winczer, Z. Phys. B64, 159 (1986).

36. Y. Kitaoka, K. Fujiwara, Y. Kohori, K. Asayama, Y. Onuki and T. Komatsubara, J. Phys. Soc. (Japan) 54, 3686 (1985).

37. L.P. Regnault, W.A.C. Erkelens, J. Rossat-Mignod, J. Flouquet, E. Walker, D. Jaccard, A. Amato and B. Hennion, "Proceedings of the International Conference on Anomalous Rare Earths and Actinides", Grenoble (1986), J. Magn. Magn. Mat., to be published.

38. Y. Onuki and T. Komatsubara, "Proceedings of the International Conference on Anomalous Rare Earths and Actinides", Grenoble (1986), J. Magn. Magn. Mat., to be published.

39. A. Sumiyama, Y. Oda, H. Nagano, Y. Onuki, T. Komatsubara, J. Phys. Soc. (Japan) 54, 877 (1985).

40. C.D. Bredl, S. Horn, F. Steglich, B. Luthi and R.M. Martin, Phys. Rev. Lett. 52, 1982 (1984).

41. G. Aeppli, H. Yoshizawa, Y. Endoh, E. Bucher, J. Hufnagl, Y. Onuki and T. Komatsubara, Phys. Rev. Lett. 57, 122 (1966).

42. T. Moriya, J. Magn. Magn. Mat. 14, 1 (1979).

43. M.T. Beal-Monod, Phys. Rev. 24, 261 (1981).

44. A. Auerbach and K. Levin, Phys. Rev. Lett. 57, 877 (1986).

45. A. Auerbach and K. Levin, Phys. Rev. 34, 3524 (1986).

46. W.H. Fogle, J.C. Ho and N.E. Phillips, J. Physique C6, 901 (1978).

47. H. Fukuyama, private communication.

48. H.E. Fisher and J.S. Lager, Phys. Rev. Lett. 20, 15 (1968).

49. A. Nakamura, N. Kawakami and A. Okiji, to be published in J. Phys. Soc. (Japan).

50. J. Flouquet, P. Haen, C. Vettier, J. Magn. Magn. Mat. 29, 159 (1982).

51. J.M. Mignot, et al., to be published. Y. Lassailly, Thesis, Grenoble 1984, and to be published.

52. U. Welp, G. Bruls, G. Remenyi, P. Haen, A. Briggs, J. Flouquet, P. Morin, G. Cors and M. Karkut, "Proceedings of the International Conference on Anomalous Rare Earths and Actinides", Grenoble (1986), J. Magn. Magn. Mat., to be published.

53. B. Luthi, et al., "Proceedings of the International Conference on Anomalous Rare Earths and Actinides", Grenoble (1986), J. Magn. Magn. Mat., to be published.

54. Y. Onuki, Y. Furukawa, T. Komatsubara, J. Phys. Soc. (Japan) 53, 2197 (1984).

55. H. Shiba, J. Phys. Soc. (Japan) 55, 2765 (1986).

56. T.V. Ramakrishnan, Phys. Rev. Lett. 48, 541 (1982).

57. P. Coleman, Phys. Rev. B28, 5255 (1983).

58. N. Read, D.M. Newns and S. Doniach, Phys. Rev. B30, 3841 (1984).

59. G. Remenyi, U. Welp, J. Flouquet, J.J.M. Franse and A. Menovski, "Proceedings of the International Conference on Rare Earths and Actinides", Grenoble (1986), J. Magn. Magn. Mat., to be published.

60. K. Hanzawa, K. Yamada and K. Yoshida, to be published in J. Phys. Soc. (Japan).

61. S. Koshiba, S. Maekawa, S. Takahashi and M. Tachiki, J. Phys. Soc. (Japan) 55, 1341 (1986).

62. D. Jaccard and J. Flouquet, to be published Helvetica Physica Acta.

63. G. Remenyi, D. Jaccard, J. Flouquet, A. Briggs, Z. Fisk, J.L. Smith and H.R. Ott, J. Physique 47, 367 (1986).

64. G. Remenyi, A. Briggs, J. Flouquet, O. Laborde and F. Lapierre, J. Magn. Magn. Mat. 31-34, 407 (1983).

65. H. Grewe, Solid State Commun. 50, 19 (1984).

66. M. Lavagna, J. Magn. Magn. Mat. 47-48, 360 (1985).

67. C. Lacroix, J. Magn. Magn. Mat. 60, 145 (1986).

68. T. Koyama and M. Tachiki, Phys. Rev. B34, 3272 (1986).

69. M. Kaveh and N. Wiser, Advances in Physics 33, 257 (1984).

70. Z. Zou and P.W. Anderson, Phys. Rev. Lett. 57, 2073 (1986).

71. A. Yoshimori and H. Kasai, J. Magn. Magn. Mat. 31-34, 475 (1983).

72. A. Yoshimori and H. Kasai, to be published in Solid State Commun.

73. M. Lavagna, Thesis, University Grenoble (1984). M. Lavagna, C. Lacroix and M. Cyrot, J. Phys. F 12, 745 (1985).

74. P. Coleman, "Proceedings of the International Conference on Rare Earths and Actinides, Grenoble (1986), J. Magn. Magn. Mat., to be published.

75. A.J. Millis and P.A. Lee, "Proceedings of the International Conference on Rare Earths and Actinides, Grenoble (1986), J. Magn. Magn. Mat., to be published.

76. K. Yamada and T. Yoshida, Prog. Theor. Phys. 76, 721 (1986).

77. S. Doniach, to be published in Phys. Rev.

78. N. Kawakami and A. Okiji, J. Phys. Soc. (Japan) 55, 2114 (1986).

79. F.J. Okhawa, J. Phys. Soc. (Japan) 55, 2527 (1986).

TABLE 1

Comparison of Parameters Characterizing HFC and IVC.

	$\chi(0)$ 10^{-4} emu/mole	γ mJmole^{-1}K^{-2}	$\gamma/\chi(0)$	Ω_{To}
		Non-Magnetic HFC		
$CeCu_6$	340	1670	0.68	81
$CeAl_3$	360	1200	0.46	-200
$CeCu_2Si_2$	180	1000	0.76	~80
$CeRu_2Si_2$	100	350	0.48	120
		Magnetic HFC		
$CeAl_2$	400	140	0.048	-10
$CeIn_3$	110	140	0.170	-5
$CePb_3$	310	1200	0.533	-27
		Non-Magnetic IVC		
$CeBe_{13}$	22	67	0.42	10
$CeSn_3$	17	42	0.34	10
$CePd_3$	15	35	0.32	10

FIGURE CAPTIONS

Figure 1. χ^{-1} vs T for $CeCu_6$ for the three principal axes.

Figure 2. Low temperature variation of χ^{-1} for $CeCu_6$ for the three principal axes. The dashed curve shows the variation of χ deduced at low temperature from specific heat measurements in magnetic fields, and the measured χ shown as a solid curve.

Figure 3. Field variation of the magnetization of $CeCu_6$ for the three principal axes at 1.1, 0.33 and 0.09K.

Figure 4. High field magnetization of $CeCu_6$ for the three principal axes at 1.6K. The insert shows the variation of M for the [001] easy magnetization axis at 1.6 and 4.2K.

Figure 5. C/T vs T at zero field. The lower insert shows a comparison of the data obtained before (sample G1) and after (sample G2) annealing. The upper insert shows the linear variation of C/T vs T at low temperatures.

Figure 6. Temperature variation of the low field ratio $C/\chi T$ vs T normalized to the free electron value.

Figure 7. Field dependence of C/T for H applied along the [100], [010] and [001] axes. The insert shows the variation of C/T with H^2 at constant T.

Figure 8. Magnetoresistivity of $CeCu_6$ at different temperatures with the current and field both along [100].

Figure 9. Magnetoresistivity of $CeCu_6$ at different temperatures with the current along the [100] and the field along the [010].

Figure 10. Magnetoresistivity of $CeCu_6$ at different temperatures with the current along the [100] and the field along the [001].

Figure 11. Temperature dependence of the resistivity at 1, 15 and 46 kOe as as function of T^2. The insert shows the field variation of the A coefficient of the quadratic T^2 dependence. The current is along the [100] and the field is along the [001].

Figure 12. Thermal conductivity and resistivity of $CeCu_6$ vs T. The insert shows the Lorentz number normalized to the free electron number.

Figure 13. Field dependence of the thermal conductivity at 287mK. The thermal gradient and the applied field are both along the [100].

Figure 14. Temperature variation of the thermoeletric power of $CeCu_6$. The insert shows the field dependence of Q at 287mK. The thermal gradient and magnetic field are both along the [100] axis.

Figure 15. Field variation of $\gamma_H \equiv \gamma(H)$, χ_H and $A_H^{1/2} \equiv A(H)^{1/2}$ as a function of H. The insert is the field variation of the ratio γ_H/χ_H. At $H = 0$, $A(H)^{1/2}$ and χ_H have been normalized to the value of $\gamma = (C/T)_{T=0}$ at H=0.

Figure 16. Phenomenological dependence of E_{int}/E_0 vs H.

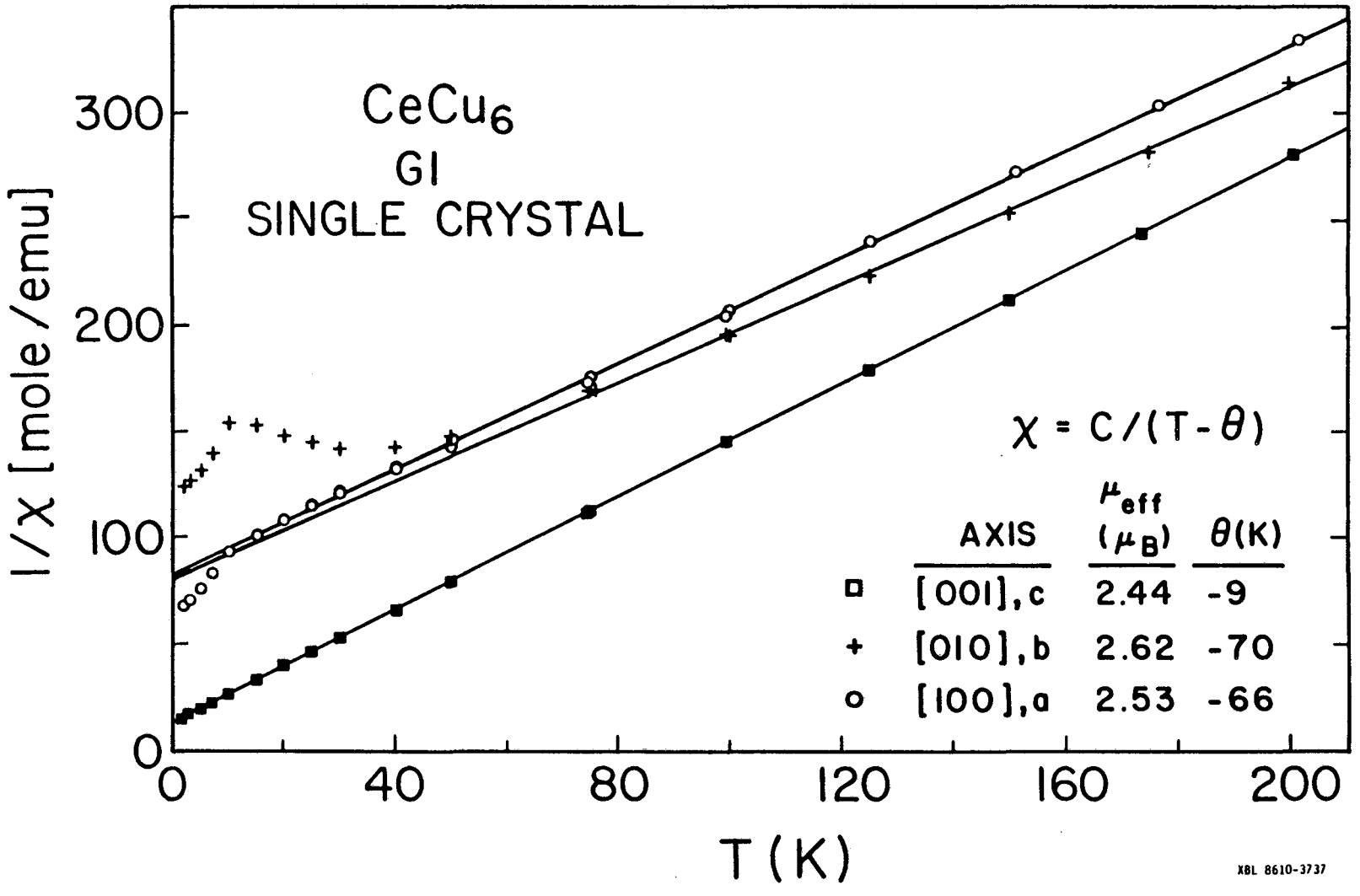
CeCu6
GI
SINGLE CRYSTAL
χ = C/(T-θ)
AXIS
μeff (μB)
θ(K)
[001],c 2.44 -9
[010],b 2.62 -70
[100],a 2.53 -66
1/χ [mole/emu]
T(K)
0
100
200
300
0
40
80
120
160
200
XBL 8610-3737

FIGURE 1

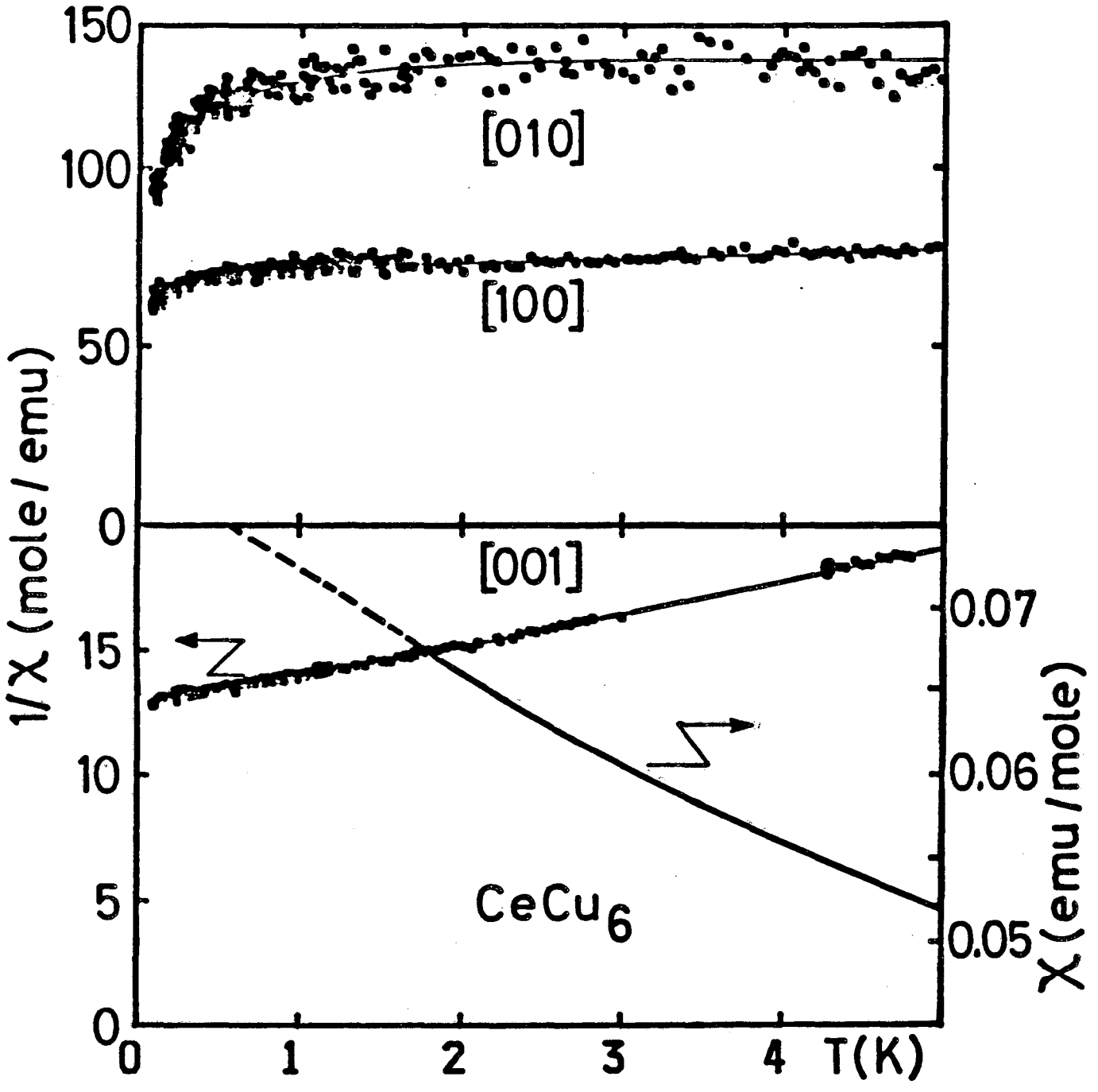
150
100
50
0
15
10
5
0
0
1
2
3
4
T(K)
[010]
[100]
[001]
CeCu6
1/χ (mole/emu)
χ (emu/mole)
0.07
0.06
0.05

FIGURE 2

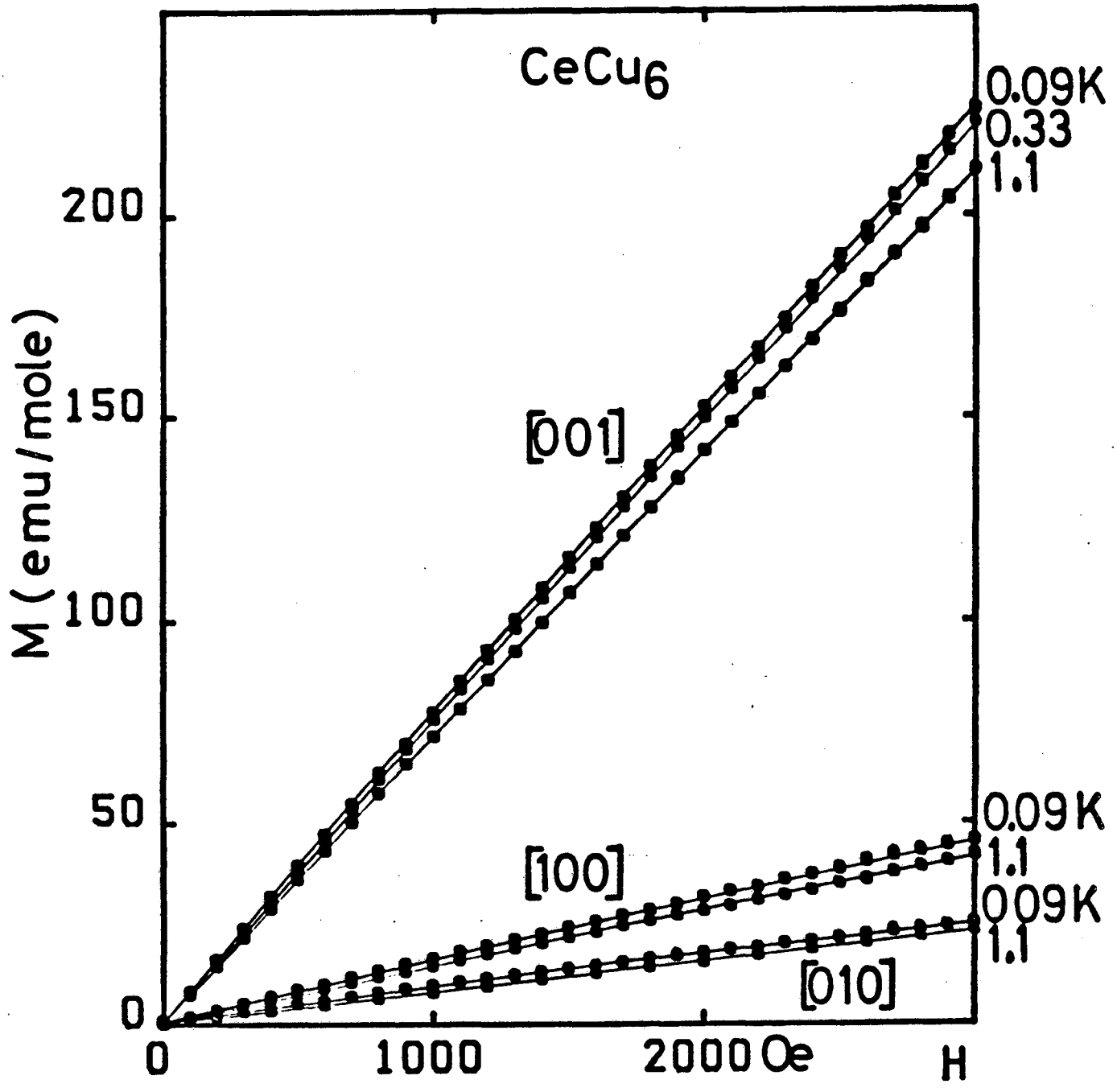
CeCu6
0.09K
0.33
1.1
200
150
100
50
0
M (emu/mole)
[001]
[100]
[010]
0.09K
1.1
0.09K
1.1
0
1000
2000 Oe
H

FIGURE 3

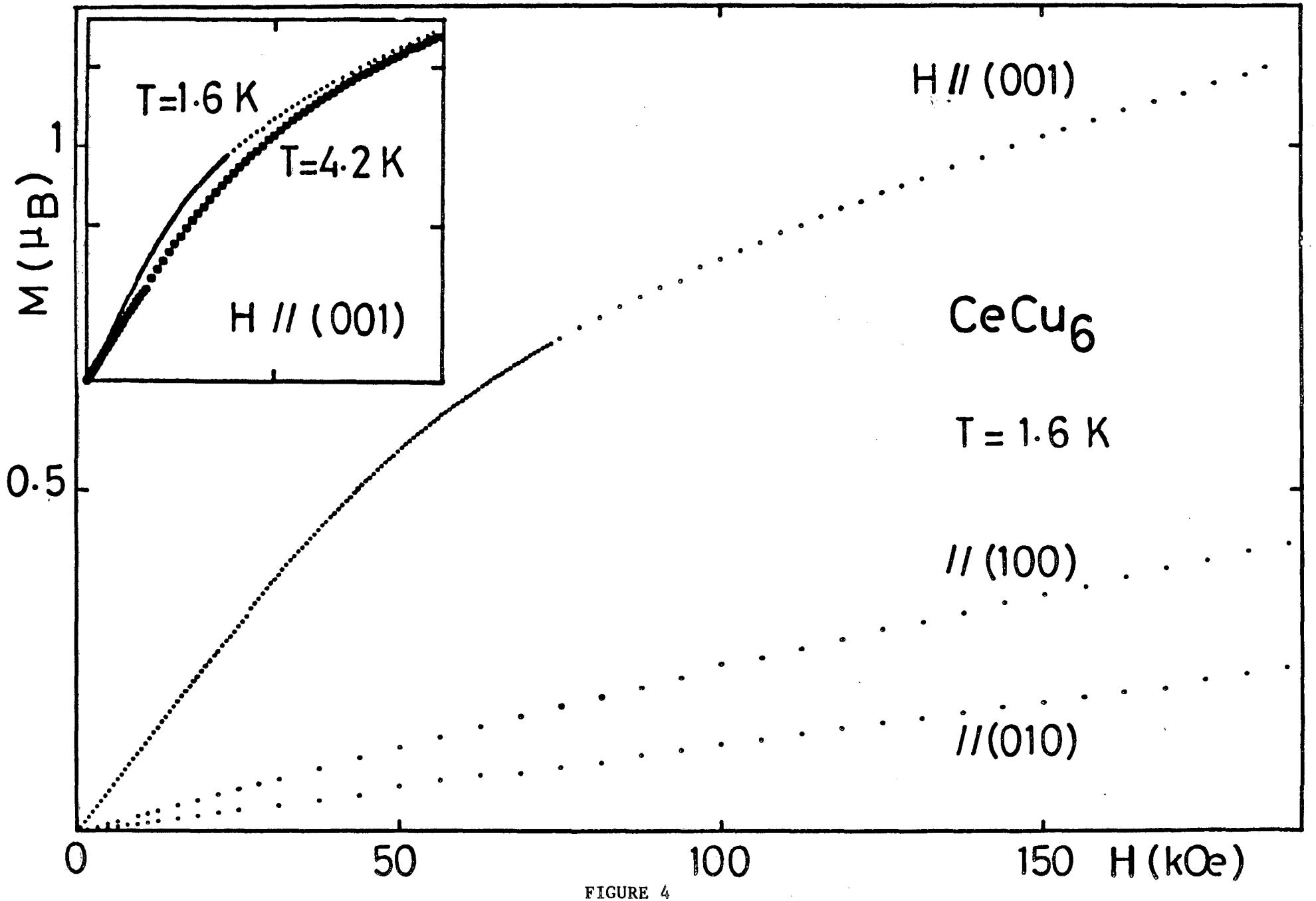
T=1.6 K
T=4.2 K
H // (001)
M (μB)
1
0.5
0
50
100
150
H (kOe)
H // (001)
CeCu6
T = 1.6 K
// (100)
//(010)

FIGURE 4

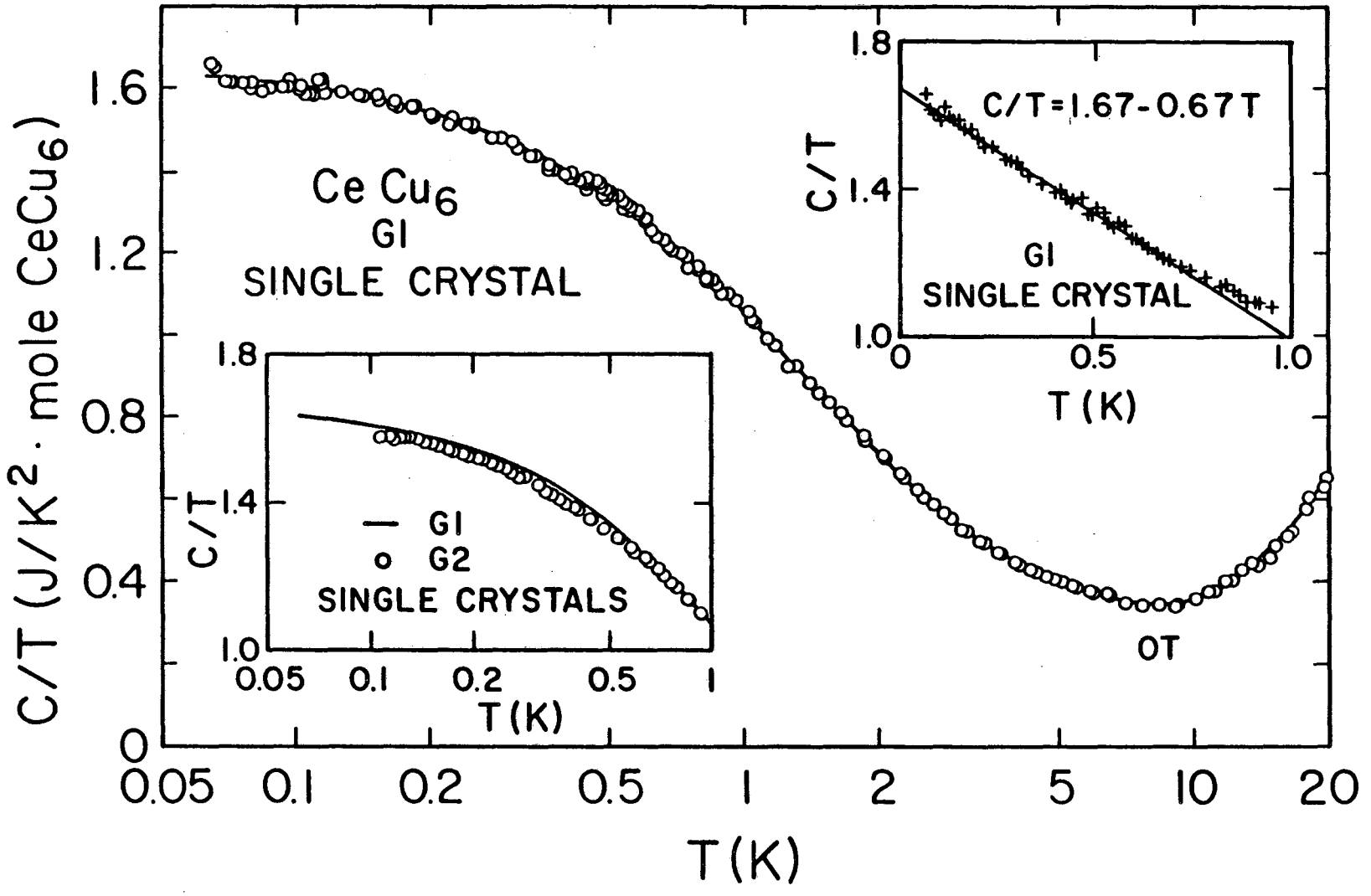

XBL 868-3092

FIGURE 5

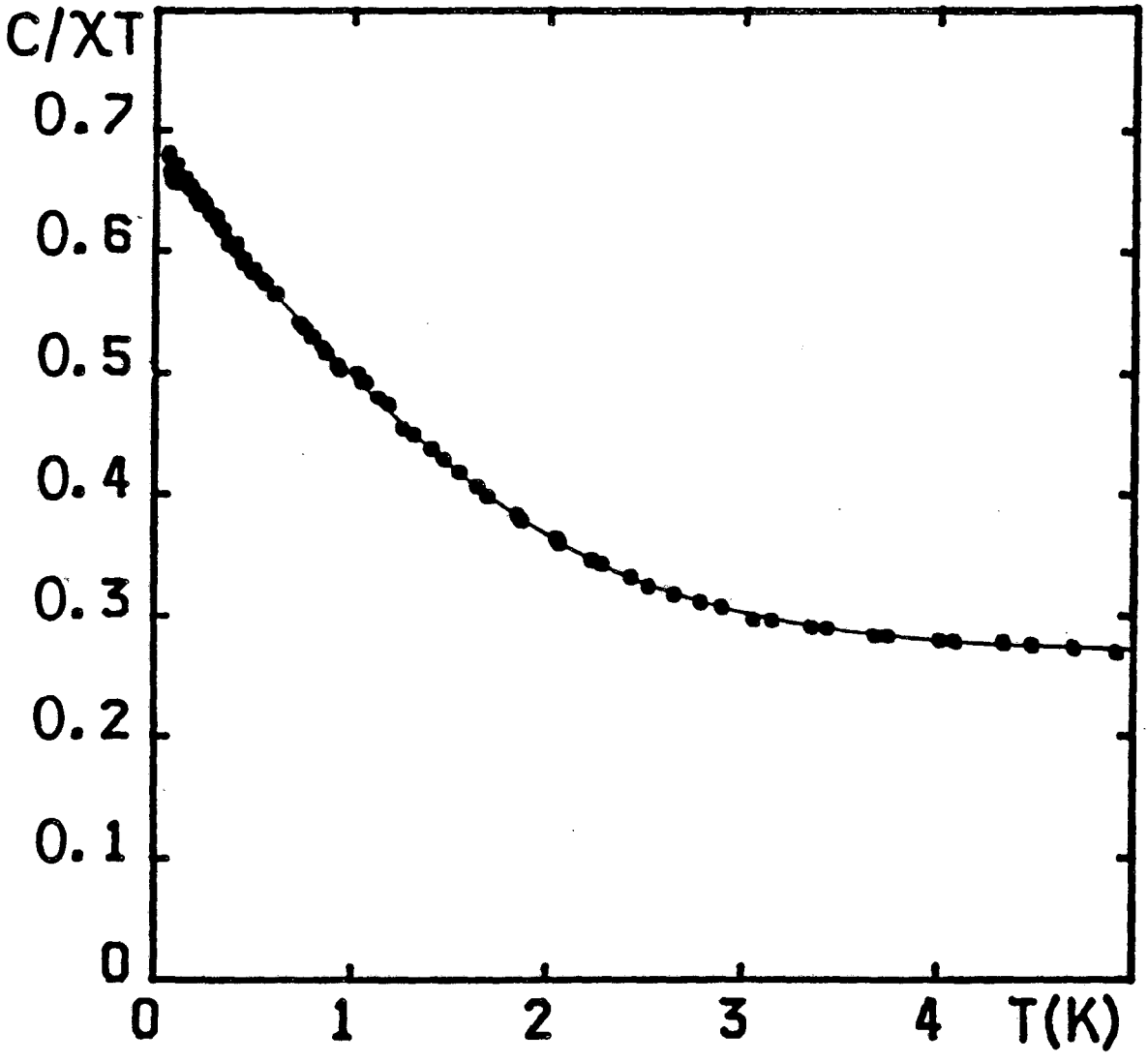

FIGURE 6

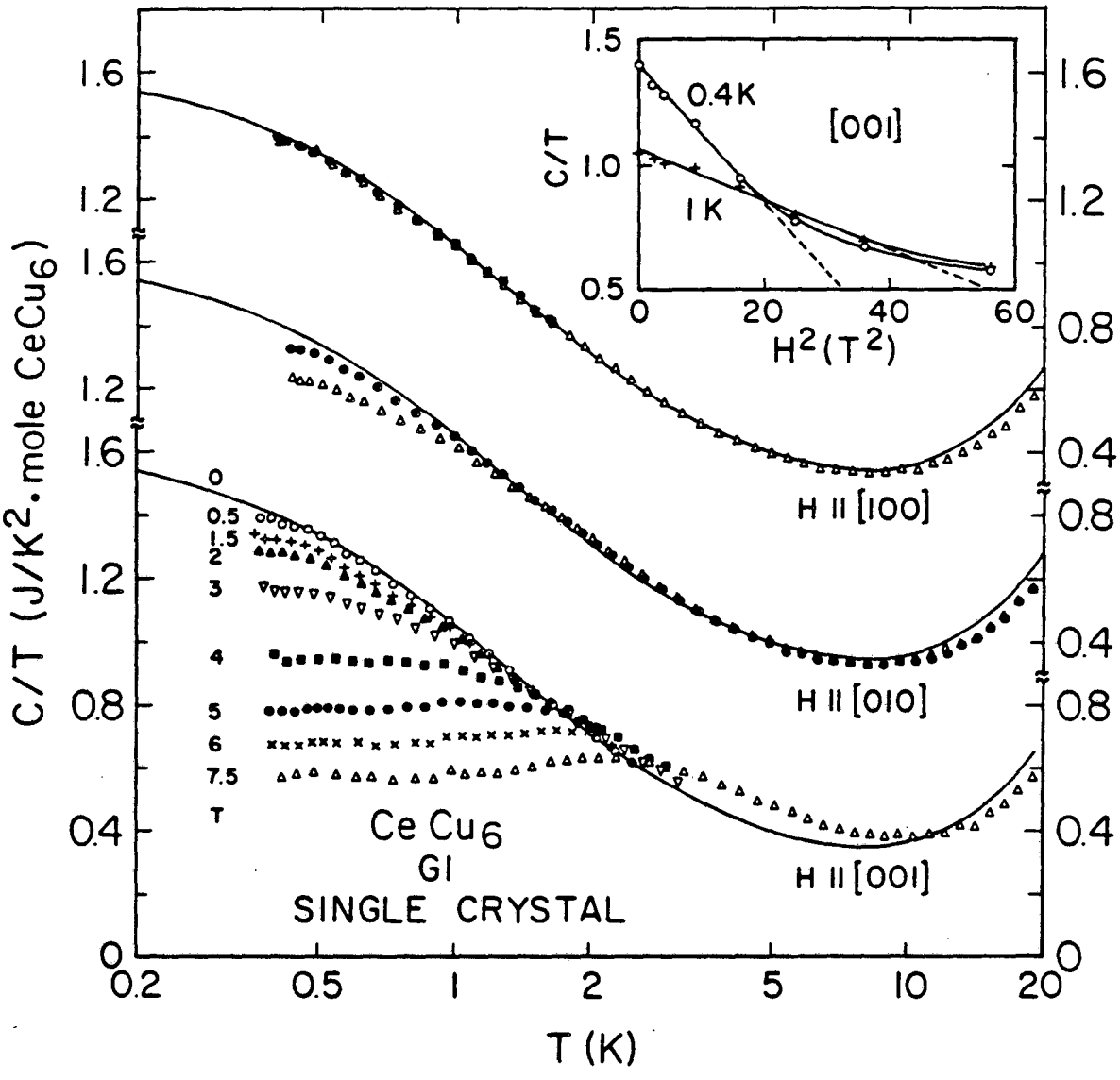

XBL 868-3094

FIGURE 7

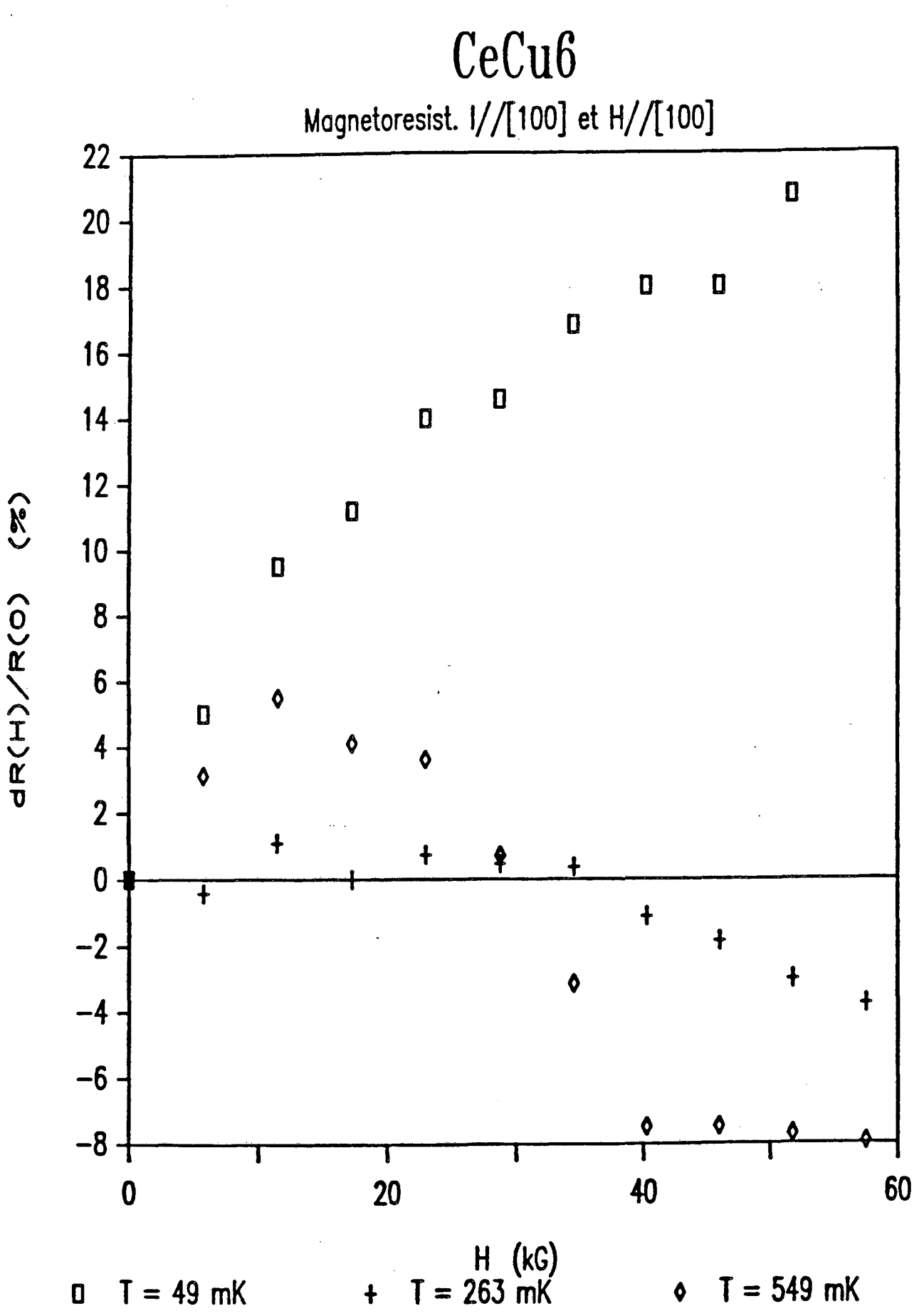
CeCu6
Magnetoresist. I//[100] et H//[100]
dR(H)/R(O) (%)
22
20
18
16
14
12
10
8
6
4
2
0
-2
-4
-6
-8
0
20
40
60
H (kG)
T = 49 mK
T = 263 mK
T = 549 mK

FIGURE 8

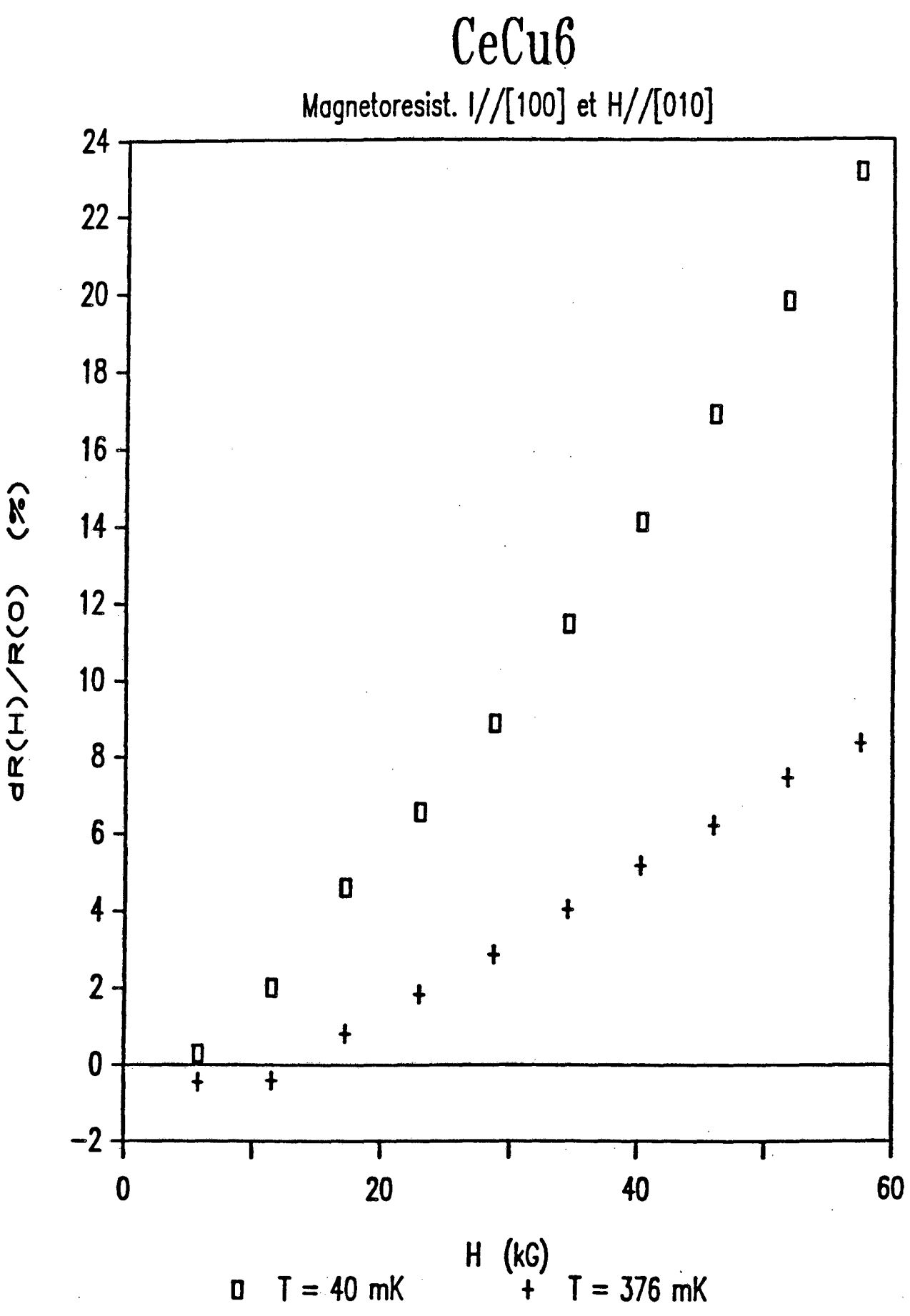
CeCu6
Magnetoresist. I//[100] et H//[010]
dR(H)/R(O) (%)
24
22
20
18
16
14
12
10
8
6
4
2
0
-2
0
20
40
60
H (kG)
T = 40 mK
T = 376 mK

FIGURE 9

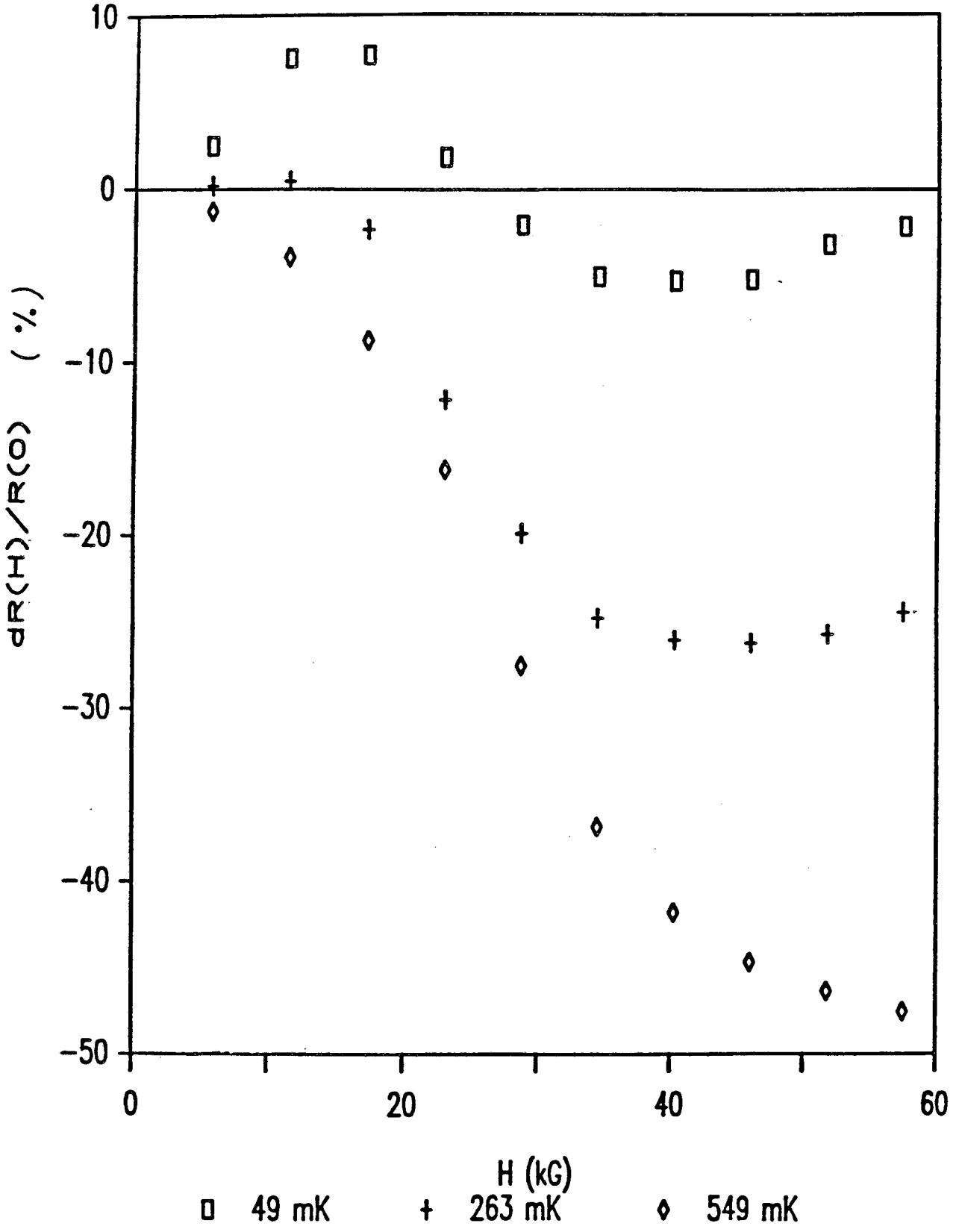
CeCu6
Magnetoresist. I//[100] et H//[001]
10
0
-10
-20
-30
-40
-50
dR(H)/R(O) (%)
0
20
40
60
H (kG)
49 mK
263 mK
549 mK

FIGURE 10

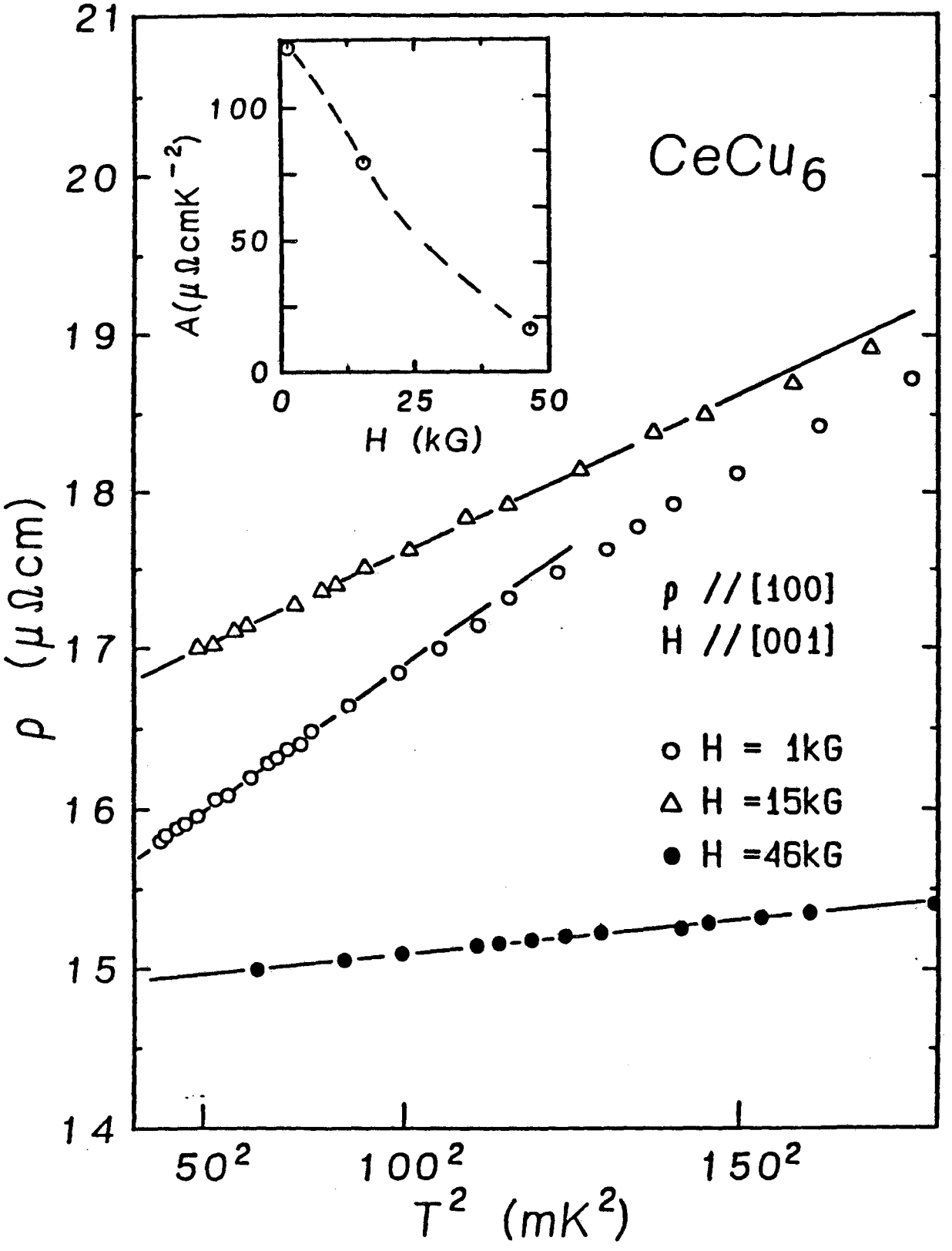
21
20
19
18
17
16
15
14
ρ (μΩcm)
50²
100²
150²
T² (mK²)
CeCu6
ρ // [100]
H // [001]
o H = 1kG
Δ H =15kG
● H =46kG
A(μΩcmK⁻²)
100
50
0
0
25
50
H (kG)

FIGURE 11

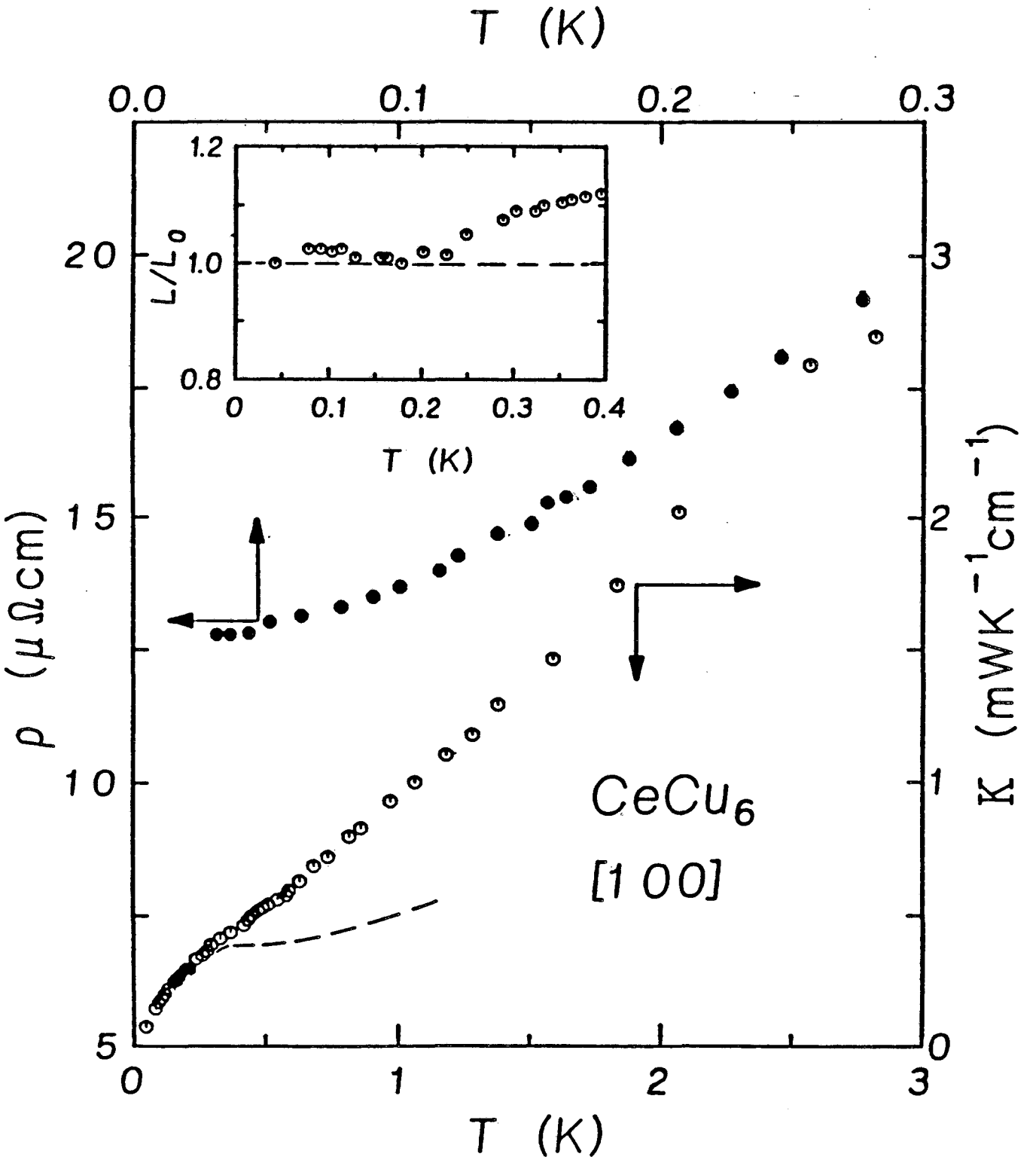
T (K)
0.0
0.1
0.2
0.3
20
15
10
5
3
2
1
0
ρ (μΩcm)
K (mWK⁻¹cm⁻¹)
0
1
2
3
T (K)
1.2
1.0
0.8
L/L₀
0
0.1
0.2
0.3
0.4
T (K)
CeCu6
[100]

FIGURE 12

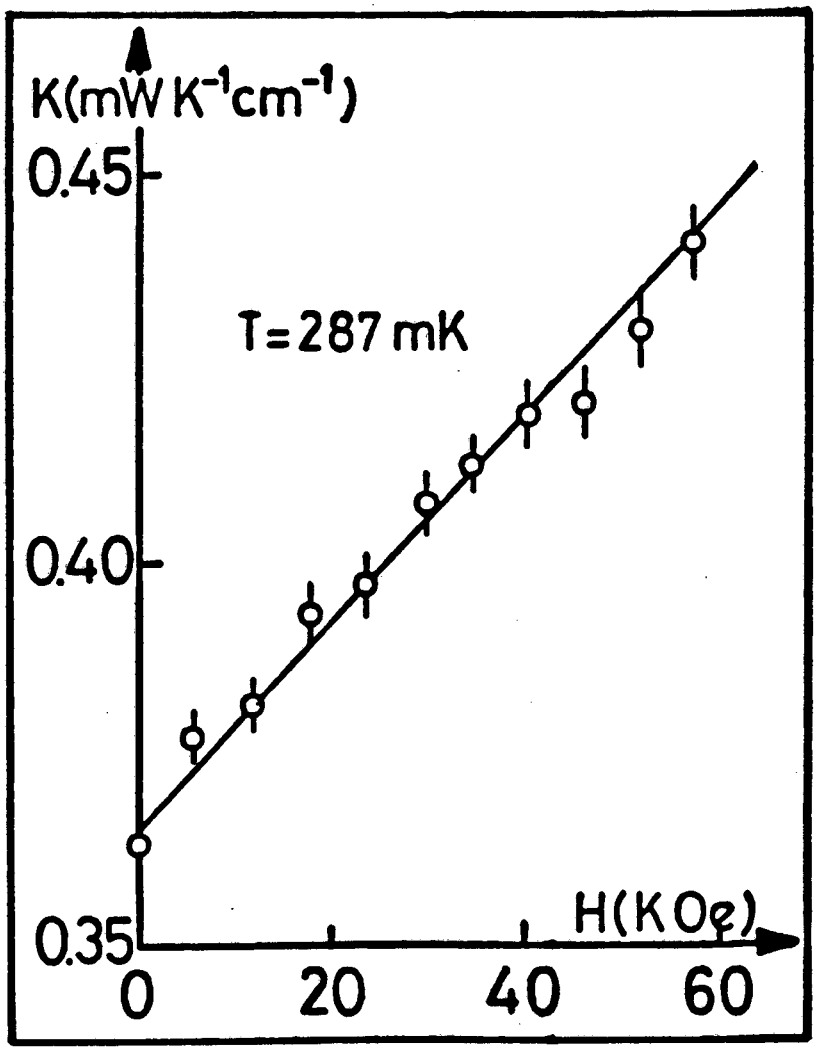

FIGURE 13

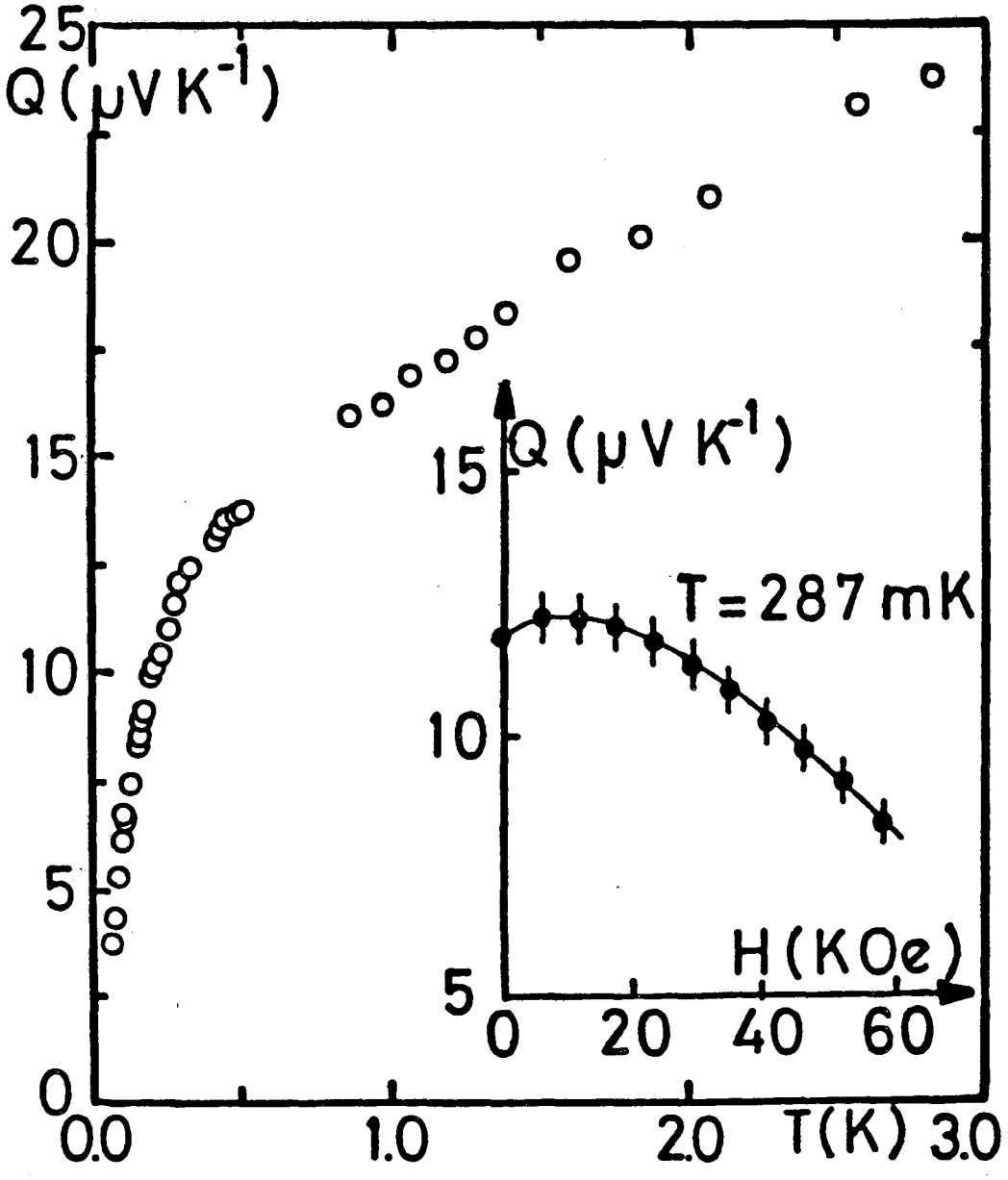
25
Q(μV K⁻¹)
20
15
10
5
0
0.0
1.0
2.0
T(K)
3.0
Q(μV K⁻¹)
15
10
5
T=287 mK
H(KOe)
0
20
40
60

FIGURE 14

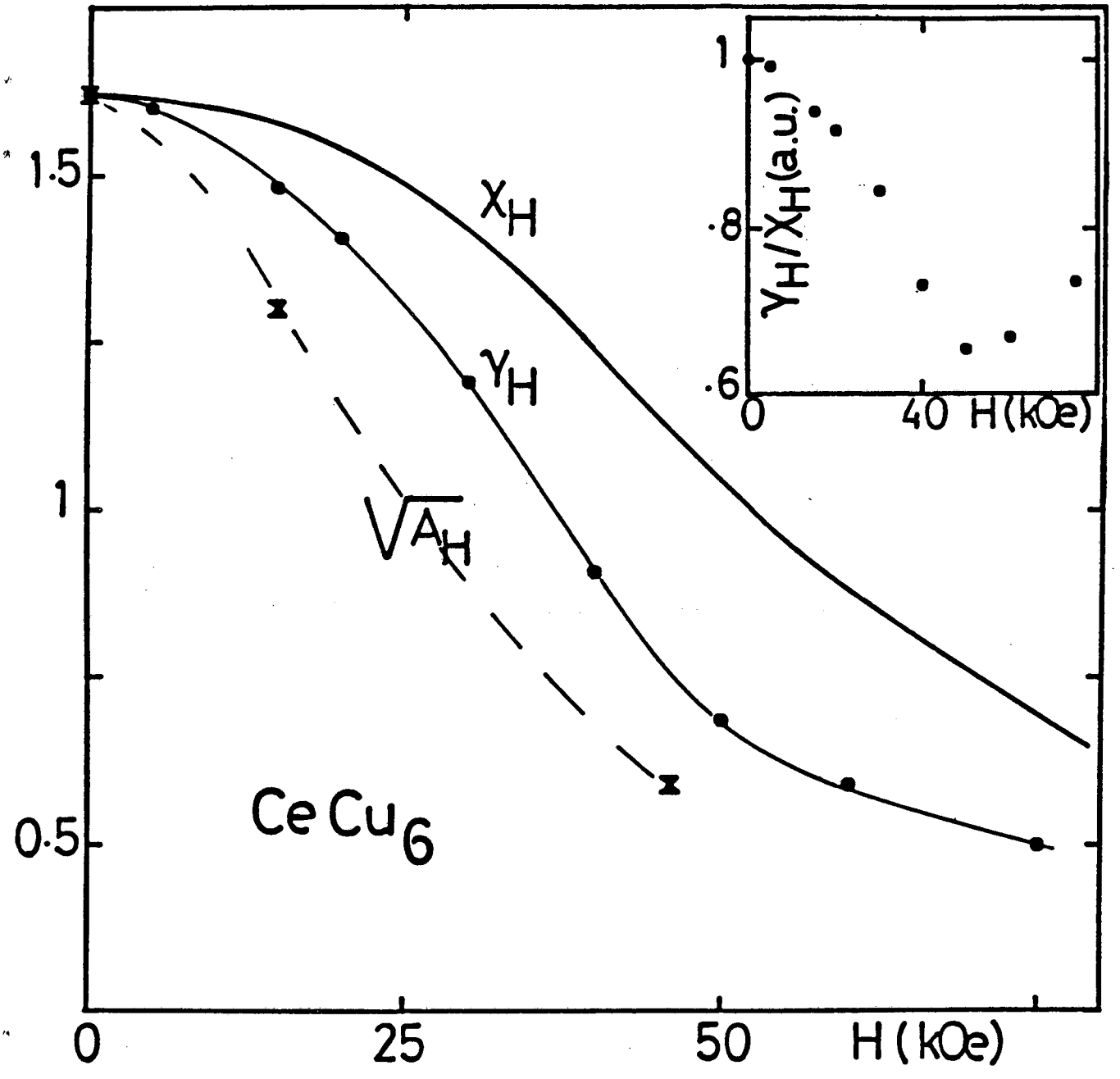
1.5
1
0.5
0
25
50
H (kOe)
χ_H
γ_H
$\sqrt{A_H}$
CeCu6
1
.8
.6
0
40 H(kOe)
γ_H/χ_H(a.u.)

FIGURE 15

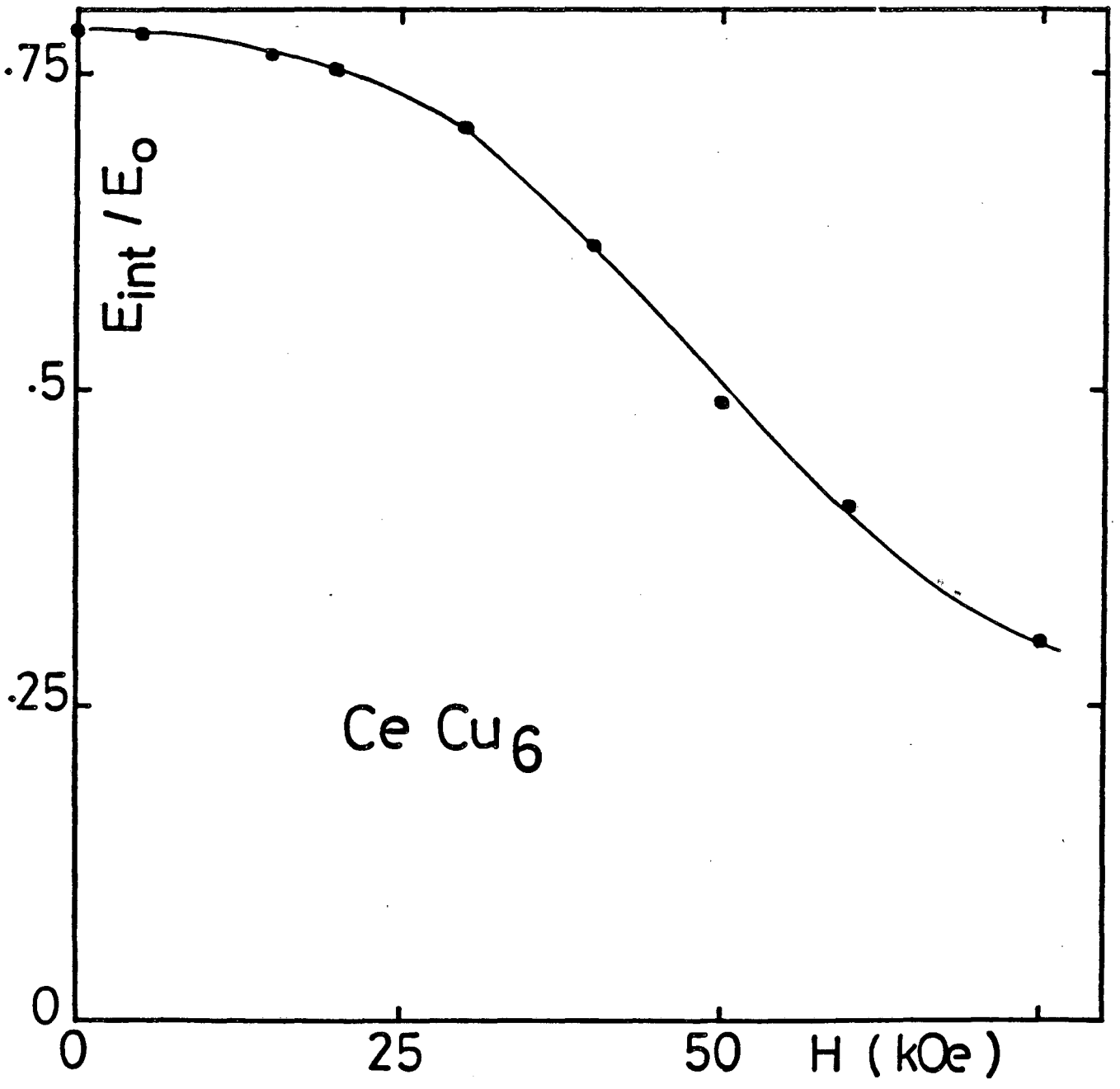

FIGURE 16

This report was done with support from the Department of Energy. Any conclusions or opinions expressed in this report represent solely those of the author(s) and not necessarily those of The Regents of the University of California, the Lawrence Berkeley Laboratory or the Department of Energy.

Reference to a company or product name does not imply approval or recommendation of the product by the University of California or the U.S. Department of Energy to the exclusion of others that may be suitable.

LAWRENCE BERKELEY LABORATORY
TECHNICAL INFORMATION DEPARTMENT
UNIVERSITY OF CALIFORNIA
BERKELEY, CALIFORNIA 94720